In conclusion, we have demonstrated that mogamulizumab shows promise as a novel treatment for HAM/TSP. Our results indicate that $CD8^+CCR4^+$ T cells and $CD4^+CCR4^+$ T cells are key therapeutic targets and, thus, that the CCR4-targeting therapy mogamulizumab can be expected to effectively ameliorate chronic inflammation in patients with HAM/TSP. The lack of success with classic antiviral therapies [8, 9] suggests that blocking viral replication is ineffective against HTLV-1, which mainly spreads by cell division [11, 12]. Targeting the infected cells themselves on the basis of their characteristic markers may be the key to combating this tricky virus. If successful, mogamulizumab would become the first treatment for a chronic viral infection that effectively targets infected cells.

Supplementary Data

Supplementary materials are available at *The Journal of Infectious Diseases* online (http://jid.oxfordjournals.org). Supplementary materials consist of data provided by the author that are published to benefit the reader. The posted materials are not copyedited. The contents of all supplementary data are the sole responsibility of the authors. Questions or messages regarding errors should be addressed to the author.

Notes

Acknowledgments. We thank M. Koike, Y. Hasegawa, Y. Suzuki-Ishikura, and Y. Saito, for technical assistance; and Kyowa Hakko Kirin, Japan, for kindly providing monoclonal antibodies (mogamulizumab and KM2760).

J. Y. performed most of the experiments, performed data analysis, created the figures, and wrote the manuscript. A. C. R. performed data interpretation and wrote the manuscript. T. S., N. A., N. Y., H. A., Y. K., and K. T. performed data analysis and interpretation. Y. T., Y. S., K. N., T. N., Y. H., A. U., and K. K. reviewed and edited the manuscript. Y. Y. developed the project, performed data analysis, and wrote the manuscript. All authors approved the final manuscript.

Financial support. This work was supported by the Ministry of Health Labor and Welfare (matching-fund subsidy for the Research on Measures for Intractable Disease project), JSPS KAKENHI (grant 25461294), and the MEXT-Supported Program for the Strategic Research Foundation at Private Universities, 2008–2012.

Potential conflicts of interest. Y. Y. has 1 established patent and another pending for the use of anti-CCR4 antibodies as a treatment for HAM/TSP. All other authors report no potential conflicts.

All authors have submitted the ICMJE Form for Disclosure of Potential Conflicts of Interest. Conflicts that the editors consider relevant to the content of the manuscript have been disclosed.

References

1. Gessain A, Barin F, Vernant JC. Antibodies to human T-lymphotropic virus type-I in patients with tropical spastic paraparesis. Lancet **1985**; 2:407–10.
2. Osame M, Usuku K, Izumo S, et al. HTLV-I associated myelopathy, a new clinical entity. Lancet **1986**; 1:1031–2.
3. Verdonck K, González E, Van Dooren S, Vandamme A, Vanham G, Gotuzzo E. Human T-lymphotropic virus 1: recent knowledge about an ancient infection. Lancet Infect Dis **2007**; 7:266–81.
4. Ijichi S, Izumo S, Eiraku N, et al. An autoaggressive process against bystander tissues in HTLV-I-infected individuals: a possible pathomechanism of HAM/TSP. Med Hypotheses **1993**; 41:542–7.
5. Nakagawa M, Nakahara K, Maruyama Y, et al. Therapeutic trials in 200 patients with HTLV-I-associated myelopathy/tropical spastic paraparesis. J Neurovirol **1996**; 2:345–55.
6. Izumo S, Goto I, Itoyama Y, et al. Interferon-alpha is effective in HTLV-I-associated myelopathy: a multicenter, randomized, double-blind, controlled trial. Neurology **1996**; 46:1016–21.
7. Olindo S, Lézin A, Cabre P, et al. HTLV-1 proviral load in peripheral blood mononuclear cells quantified in 100 HAM/TSP patients: a marker of disease progression. J Neurol Sci **2005**; 237:53–9.
8. Taylor GP, Goon P, Furukawa Y, et al. Zidovudine plus lamivudine in human T-lymphotropic virus type-l-associated myelopathy: A randomised trial. Retrovirology **2006**; 3:63.
9. Macchi B, Balestrieri E, Ascolani A, et al. Susceptibility of primary HTLV-1 isolates from patients with HTLV-1-associated myelopathy to reverse transcriptase inhibitors. Viruses **2011**; 3:469–83.
10. De Clercq E. A cutting-edge view on the current state of antiviral drug development. Med Res Rev **2013**; 33:1249–77.
11. Wattel E, Vartanian JP, Pannetier C, Wain-Hobson S. Clonal expansion of human T-cell leukemia virus type I-infected cells in asymptomatic and symptomatic carriers without malignancy. J Virol **1995**; 69:2863–8.
12. Cavrois M, Leclercq I, Gout O, Gessain A, Wain-Hobson S, Wattel E. Persistent oligoclonal expansion of human T-cell leukemia virus type 1-infected circulating cells in patients with tropical spastic paraparesis/HTLV-1 associated myelopathy. Oncogene **1998**; 17:77–82.
13. Ishida T, Joh T, Uike N, et al. Defucosylated anti-CCR4 monoclonal antibody (KW-0761) for relapsed adult T-cell leukemia-lymphoma: a multicenter phase II study. J Clin Oncol **2012**; 30:837–42.
14. Ishida T, Utsunomiya A, Iida S, et al. Clinical significance of CCR4 expression in adult T-cell leukemia/lymphoma: its close association with skin involvement and unfavorable outcome. Clin Cancer Res **2003**; 9:3625–34.
15. Niwa R, Shoji-Hosaka E, Sakurada M, et al. Defucosylated chimeric anti-CC chemokine receptor 4 IgG1 with enhanced antibody-dependent cellular cytotoxicity shows potent therapeutic activity to T-cell leukemia and lymphoma. Cancer Res **2004**; 64:2127–33.
16. Ishii T, Ishida T, Utsunomiya A, et al. Defucosylated humanized anti-CCR4 monoclonal antibody KW-0761 as a novel immunotherapeutic agent for adult T-cell leukemia/lymphoma. Clin Cancer Res **2010**; 16:1520–31.
17. Yamano Y, Araya N, Sato T, et al. Abnormally high levels of virus-infected IFN-γ+CCR4+CD4+CD25+ T cells in a retrovirus-associated neuroinflammatory disorder. PLoS One **2009**; 4:e6517.
18. Araya N, Sato T, Ando H, et al. HTLV-1 induces a Th1-like state in CD4+CCR4+ T cells. J Clin Invest **2014**; 124:3431–42.
19. Nagai M, Brennan MB, Sakai JA, Mora CA, Jacobson S. CD8(+) T cells are an in vivo reservoir for human T-cell lymphotropic virus type I. Blood **2001**; 98:1858–61.
20. Inaoki M, Sato S, Shirasaki F, Mukaida N, Takehara K. The frequency of type 2 CD8+ T cells is increased in peripheral blood from patients with psoriasis vulgaris. J Clin Immunol **2003**; 23:269–78.
21. Cho BA, Sim JH, Park JA, et al. Characterization of effector memory CD8+ T cells in the synovial fluid of rheumatoid arthritis. J Clin Immunol **2012**; 32:709–20.
22. Hieshima K, Nagakubo D, Nakayama T, Shirakawa A, Jin Z, Yoshie O. Tax-inducible production of CC chemokine ligand 22 by human T cell leukemia virus type 1 (HTLV-1)-infected T cells promotes preferential transmission of HTLV-1 to CCR4-expressing CD4+ T cells. J Immunol **2008**; 180:931–9.
23. Osame M. Review of WHO Kagoshima meeting and diagnostic guidelines for HAM/TSP. In: Blattner WA, ed. Human retrovirology: HTLV. New York: Raven Press, **1990**: 191–7.
24. Yamano Y, Nagai M, Brennan M, et al. Correlation of human T-cell lymphotropic virus type 1 (HTLV-1) mRNA with proviral DNA load, virus-specific CD8+ T cells, and disease severity in HTLV-1-associated myelopathy (HAM/TSP). Blood **2002**; 99:88–94.
25. Lee B, Tanaka Y, Tozawa H. Monoclonal antibody defining tax protein of human T-cell leukemia virus type-I. Tohoku J Exp Med **1989**; 157:1–11.
26. Itoyama Y, Minato S, Kira J, et al. Spontaneous proliferation of peripheral blood lymphocytes increased in patients with HTLV-I-associated myelopathy. Neurology **1988**; 38:1302–7.

27. Tanner A, Bochner F, Caffin J, Halliday J, Powell L. Dose-dependent prednisolone kinetics. Clin Pharmacol Ther **1979**; 25:571–8.
28. Toulza F, Heaps A, Tanaka Y, Taylor GP, Bangham CR. High frequency of CD4+FoxP3+ cells in HTLV-1 infection: inverse correlation with HTLV-1-specific CTL response. Blood **2008**; 111:5047–53.
29. Shimizu Y, Takamori A, Utsunomiya A, et al. Impaired Tax-specific T-cell responses with insufficient control of HTLV-1 in a subgroup of individuals at asymptomatic and smoldering stages. Cancer Sci **2009**; 100:481–9.
30. Ando H, Sato T, Tomaru U, et al. Positive feedback loop via astrocytes causes chronic inflammation in virus-associated myelopathy. Brain **2013**; 136:2876–87.
31. Machigashira K, Ijichi S, Nagai M, Yamano Y, Hall WW, Osame M. In vitro virus propagation and high cellular responsiveness to the infected cells in patients with HTLV-I-associated myelopathy (HAM/TSP). J Neurol Sci **1997**; 149:141–5.
32. Sakai JA, Nagai M, Brennan MB, Mora CA, Jacobson S. In vitro spontaneous lymphoproliferation in patients with human T-cell lymphotropic virus type I-associated neurologic disease: predominant expansion of CD8+ T cells. Blood **2001**; 98:1506–11.
33. Nagai M, Usuku K, Matsumoto W, et al. Analysis of HTLV-I proviral load in 202 HAM/TSP patients and 243 asymptomatic HTLV-I carriers: high proviral load strongly predisposes to HAM/TSP. J Neurovirol **1998**; 4:586–93.
34. Iwanaga M, Watanabe T, Utsunomiya A, et al. Human T-cell leukemia virus type I (HTLV-1) proviral load and disease progression in asymptomatic HTLV-1 carriers: a nationwide prospective study in Japan. Blood **2010**; 116:1211–9.
35. Geginat J, Lanzavecchia A, Sallusto F. Proliferation and differentiation potential of human CD8+ memory T-cell subsets in response to antigen or homeostatic cytokines. Blood **2003**; 101:4260–6.
36. Kondo T, Takiguchi M. Human memory CCR4+CD8+ T cell subset has the ability to produce multiple cytokines. Int Immunol **2009**; 21: 523–32.
37. Baek HJ, Zhang L, Jarvis LB, Gaston JS. Increased IL-4+ CD8+ T cells in peripheral blood and autoreactive CD8+ T cell lines of patients with inflammatory arthritis. Rheumatology (Oxford) **2008**; 47:795–803.
38. Nagai M, Kubota R, Greten TF, Schneck JP, Leist TP, Jacobson S. Increased activated human T cell lymphotropic virus Type I (HTLV-I) Tax11–19-specific memory and effector CD8+ cells in patients with HTLV-I-associated myelopathy/tropical spastic paraparesis: correlation with HTLV-I provirus load. J Infect Dis **2001**; 183:197–205.
39. Yasunaga J, Sakai T, Nosaka K, et al. Impaired production of naive T lymphocytes in human T-cell leukemia virus type I-infected individuals: its implications in the immunodeficient state. Blood **2001**; 97:3177–83.
40. Joshi NS, Cui W, Chandele A, et al. Inflammation directs memory precursor and short-lived effector CD8+ T cell fates via the graded expression of T-bet transcription factor. Immunity **2007**; 27:281–95.
41. Kannagi M, Hasegawa A, Kinpara S, Shimizu Y, Takamori A, Utsunomiya A. Double control systems for human T-cell leukemia virus type 1 by innate and acquired immunity. Cancer Sci **2011**; 102:670–6.
42. Hanon E, Hall S, Taylor GP, et al. Abundant tax protein expression in CD4+ T cells infected with human T-cell lymphotropic virus type I (HTLV-I) is prevented by cytotoxic T lymphocytes. Blood **2000**; 95: 1386–92.
43. Vine AM, Heaps AG, Kaftantzi L, et al. The role of CTLs in persistent viral infection: cytolytic gene expression in CD8+ lymphocytes distinguishes between individuals with a high or low proviral load of human T cell lymphotropic virus type 1. J Immunol **2004**; 173:5121–9.
44. Hanon E, Stinchcombe JC, Saito M, et al. Fratricide among CD8+ T lymphocytes naturally infected with human T cell lymphotropic virus type I. Immunity **2000**; 13:657–64.
45. Sugiyama D, Nishikawa H, Maeda Y, et al. Anti-CCR4 mAb selectively depletes effector-type FoxP3+CD4+ regulatory T cells, evoking antitumor immune responses in humans. Proc Natl Acad Sci U S A **2013**; 110:17945–50.
46. Ishida T, Ueda R. Immunopathogenesis of lymphoma: focus on CCR4. Cancer Sci **2011**; 102:44–50.

The Journal of Clinical Investigation RESEARCH ARTICLE

HTLV-1 induces a Th1-like state in CD4+CCR4+ T cells

Natsumi Araya,[1] Tomoo Sato,[1] Hitoshi Ando,[1] Utano Tomaru,[2] Mari Yoshida,[3] Ariella Coler-Reilly,[1] Naoko Yagishita,[1] Junji Yamauchi,[1] Atsuhiko Hasegawa,[4] Mari Kannagi,[4] Yasuhiro Hasegawa,[5] Katsunori Takahashi,[1] Yasuo Kunitomo,[1] Yuetsu Tanaka,[6] Toshihiro Nakajima,[7,8] Kusuki Nishioka,[7] Atae Utsunomiya,[9] Steven Jacobson,[10] and Yoshihisa Yamano[1]

[1]Department of Rare Diseases Research, Institute of Medical Science, St. Marianna University School of Medicine, Kanagawa, Japan. [2]Department of Pathology, Hokkaido University Graduate School of Medicine, Hokkaido, Japan. [3]Institute for Medical Science of Aging, Aichi Medical University, Aichi, Japan. [4]Department of Immunotherapeutics, Tokyo Medical and Dental University, Graduate School, Tokyo, Japan. [5]Department of Neurology, St. Marianna University School of Medicine, Kanagawa, Japan. [6]Department of Immunology, Graduate School of Medicine, University of the Ryukyus, Okinawa, Japan. [7]Institute of Medical Science and [8]Center for Clinical Research, Tokyo Medical University, Tokyo, Japan. [9]Department of Hematology, Imamura Bun-in Hospital, Kagoshima, Japan. [10]Viral Immunology Section, Neuroimmunology Branch, National Institutes of Health, Bethesda, Maryland, USA.

Human T-lymphotropic virus type 1 (HTLV-1) is linked to multiple diseases, including the neuroinflammatory disease HTLV-1–associated myelopathy/tropical spastic paraparesis (HAM/TSP) and adult T cell leukemia/lymphoma. Evidence suggests that HTLV-1, via the viral protein Tax, exploits CD4+ T cell plasticity and induces transcriptional changes in infected T cells that cause suppressive CD4+CD25+CCR4+ Tregs to lose expression of the transcription factor FOXP3 and produce IFN-γ, thus promoting inflammation. We hypothesized that transformation of HTLV-1–infected CCR4+ T cells into Th1-like cells plays a key role in the pathogenesis of HAM/TSP. Here, using patient cells and cell lines, we demonstrated that Tax, in cooperation with specificity protein 1 (Sp1), boosts expression of the Th1 master regulator T box transcription factor (T-bet) and consequently promotes production of IFN-γ. Evaluation of CSF and spinal cord lesions of HAM/TSP patients revealed the presence of abundant CD4+CCR4+ T cells that coexpressed the Th1 marker CXCR3 and produced T-bet and IFN-γ. Finally, treatment of isolated PBMCs and CNS cells from HAM/TSP patients with an antibody that targets CCR4+ T cells and induces cytotoxicity in these cells reduced both viral load and IFN-γ production, which suggests that targeting CCR4+ T cells may be a viable treatment option for HAM/TSP.

Introduction

The flexibility of the CD4+ T cell differentiation program that underlies the success of the adaptive immune response has recently been implicated in the pathogeneses of numerous inflammatory diseases (1–3). The majority of CD4+ T lymphocytes belong to a class of cells known as Th cells, so called because they provide help on the metaphorical immune battlefield by stimulating the other soldiers — namely, B cells and cytotoxic T lymphocytes — via secretion of various cytokines. Interestingly, there is also a minority group of CD4+ T cells with quite the opposite function: Tregs actively block immune responses by suppressing the activities of CD4+ Th cells as well as many other leukocytes (4). Tregs are credited with maintaining immune tolerance and preventing inflammatory diseases that could otherwise occur as a result of uninhibited immune reactions (5). Thus, the up- or downregulation of certain CD4+ T cell lineages could disrupt the carefully balanced immune system, threatening bodily homeostasis.

The plasticity of CD4+ T cells, particularly Tregs, makes CD4+ T cell lineages less clean-cut than they may originally appear. CD4+ T cells are subdivided according to various lineage-specific chemokine receptors and transcription factors they express, as well as the cytokines they produce (6). Th1 cells, for example, can be identified by expression of CXC motif receptor 3 (CXCR3) and T box transcription factor (T-bet; encoded by *TBX21*) and are known to secrete the proinflammatory cytokine IFN-γ (6). While both have been known to express CC chemokine receptor 4 (CCR4) and CD25, Th2 cells and Tregs can usually be distinguished from each other by their expression of GATA-binding protein 3 (GATA3) and forkhead box p3 (FOXP3), respectively (6, 7). CCR4 is coexpressed in the majority of CD4+FOXP3+ cells and in virtually all CD4+CD25+FOXP3+ cells, making it a useful — albeit not fully specific — marker for Tregs (8, 9). FOXP3 is a particularly noteworthy marker because its expression is said to be required for Treg identity and function (10). In fact, *Foxp3* point mutations are reported to cause fatal multiorgan autoimmune diseases (11). Even partial loss of FOXP3 expression can disrupt the suppressive nature of Tregs, representing one of several pathways by which even fully differentiated Tregs can reprogram into inflammatory cells (12). There have been several reports of Tregs reprogramming in response to proinflammatory cytokines such as IL-1, IL-6, IL-12, and IFN-γ (12, 13); it is thought that this reprogramming may have evolved as an adaptive mechanism for dampening immune suppression when protective inflammation is necessary (12). However, this same plasticity can lead to pathologically chronic inflammation, and several autoimmune diseases have been associated with reduced FOXP3 expression and/or Treg function, including multiple sclerosis, myasthenia gravis, and type 1 diabetes (14, 15).

Of the roughly 10–20 million people worldwide infected with human T-lymphotropic virus type 1 (HTLV-1), up to 2%–3% are affected by the neurodegenerative chronic inflammatory dis-

Conflict of interest: The authors have declared that no conflict of interest exists.
Submitted: January 17, 2014; **Accepted:** May 8, 2014.
Reference information: *J Clin Invest.* 2014;124(8):3431–3442. doi:10.1172/JCI75250.

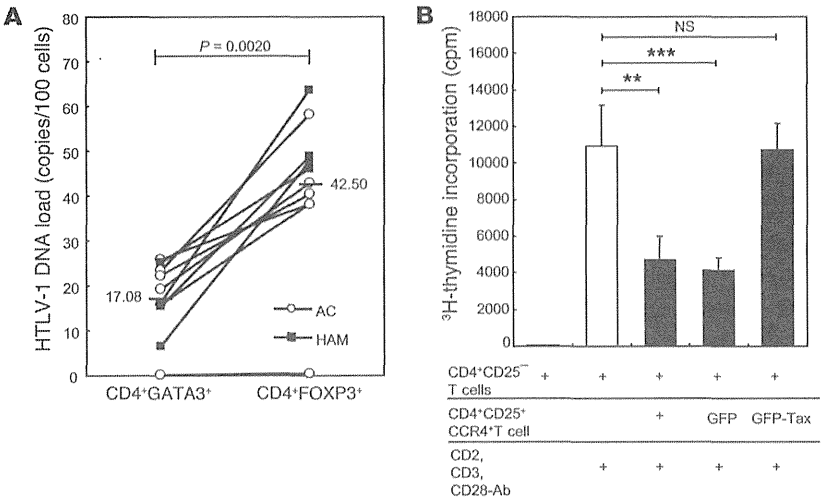

Figure 1. HTLV-1 mainly infects Tregs and inhibits their regulatory function. (**A**) Higher HTLV-1 proviral DNA load in CD4⁺FOXP3⁺ cells (Tregs) compared with CD4⁺GATA3⁺ cells ($P = 0.0020$, Wilcoxon test) from asymptomatic carriers (AC; $n = 6$) and HAM/TSP patients ($n = 4$). PBMCs were FACS sorted, and proviral load was measured using quantitative PCR. Horizontal bars represent the mean value for each set. (**B**) Loss of regulatory function in Tax-expressing CD4⁺CD25⁺CCR4⁺ cells (Tregs). CD4⁺CD25⁻ T cells from an HD were stimulated with CD2, CD3, and CD28 antibodies and cultured alone or in the presence of equal numbers of CD4⁺CD25⁺CCR4⁺ T cells, GFP lentivirus–infected HD CD4⁺CD25⁺CCR4⁺ T cells, or GFP-Tax lentivirus–infected HD CD4⁺CD25⁺CCR4⁺ T cells. As a control, CD4⁺CD25⁻ T cells alone were cultured without any stimulus. Proliferation of T cells was determined using ^{3}H-thymidine incorporation by adding ^{3}H-thymidine for 16 hours after 4 days of culture. All tests were performed in triplicate. Data are mean ± SD. $^{**}P < 0.01$, $^{***}P < 0.001$, ANOVA followed by Tukey test for multiple comparisons.

ease HTLV-1–associated myelopathy/tropical spastic paraparesis (HAM/TSP). The main other condition associated with the retrovirus is adult T cell leukemia/lymphoma (ATLL), a rare and aggressive cancer of the T cells. HAM/TSP represents a useful starting point from which to investigate the origins of chronic inflammation, because the primary cause of the disease — viral infection — is so unusually well defined. HAM/TSP patients share many immunological characteristics with FOXP3 mutant mice, including multiorgan lymphocytic infiltrates, overproduction of inflammatory cytokines, and spontaneous lymphoproliferation of cultured CD4⁺ T cells (16–18). We and others have proposed that HTLV-1 preferentially infects CD4⁺CD25⁺CCR4⁺ T cells, a group that includes Tregs (7, 19). Samples of CD4⁺CD25⁺CCR4⁺ T cells isolated from HAM/TSP patients exhibited low FOXP3 expression as well as reduced production of suppressive cytokines and low overall suppressive ability — in fact, these CD4⁺CD25⁺CCR4⁺FOXP3⁻ T cells were shown to produce IFN-γ and express Ki67, a marker of cell proliferation (19). The frequency of these IFN-γ–producing CD4⁺CD25⁺CCR4⁺ T cells in HAM/TSP patients was correlated with disease severity (19). Finally, evidence suggests that the HTLV-1 protein product Tax may play a role in this alleged transformation of Tregs into proinflammatory cells in HAM/TSP patients: transfecting Tax into CD4⁺CD25⁺ cells from healthy donors (HDs) reduced FOXP3 mRNA expression, and Tax expression in CD4⁺CD25⁺CCR4⁺ cells was higher in HAM/TSP versus ATLL patients despite similar proviral loads (19, 20). Therefore, we hypothesized that HTLV-1 causes chronic inflammation by infecting CD4⁺CD25⁺CCR4⁺ T cells and inducing their transformation into Th1-like, IFN-γ–producing proinflammatory cells via intracellular Tax expression and subsequent transcriptional alterations including but not limited to loss of endogenous FOXP3 expression.

In this study, we first sought to discover the detailed mechanism by which Tax influences the function of CD4⁺CD25⁺CCR4⁺ T cells. We used DNA microarray analysis of CD4⁺CD25⁺CCR4⁺ T cells from HAM/TSP patients to identify *TBX21*, known as a master transcription factor for Th1 differentiation, as a key intermediary between Tax expression and IFN-γ production. We demonstrated that Tax, in concert with specificity protein 1 (Sp1), amplified *TBX21* transcription and subsequently IFN-γ production. Next, we established the presence of Th1-like CD4⁺CCR4⁺ T cells in the CSF and spinal cord lesions of HAM/TSP patients. The majority of these CD4⁺CCR4⁺ T cells coexpressed CXCR3 as well as T-bet and IFN-γ. Finally, we investigated the therapeutic potential of an anti-CCR4 monoclonal antibody with antibody-dependent cellular cytotoxicity (ADCC) (21). Applying this antibody in vitro diminished the proliferative capacity of cultured PBMCs and reduced both proviral DNA load and IFN-γ production in cultured CSF cells as well as PBMCs. In conclusion, we were able to elucidate a more detailed mechanism for the pathogenesis of HAM/TSP and use our findings to suggest a possible therapeutic strategy.

Results

HTLV-1 preferentially infects Tregs and alters their behavior via Tax. Experiments were conducted to determine which among CD4⁺CD25⁺CCR4⁺ T cells were infected by HTLV-1, and how the infection influenced their functionality. Analysis of fluorescence-activated cell sorting (FACS)-sorted PBMCs obtained from asymptomatic carriers ($n = 6$) as well as HAM/TSP patients ($n = 4$) revealed that Tregs (CD4⁺FOXP3⁺) carried much higher proviral loads than Th2 cells (CD4⁺GATA3⁺) ($P = 0.0020$; Figure 1A). As it is well established that each infected cell contains only 1 copy of the HTLV-1 provirus (22, 23), these results indicate that a larger proportion of FOXP3⁺ than GATA3⁺ CD4⁺ T cells are infected. As expected, proliferation of CD4⁺CD25⁻ cells after stimulation, as measured by ^{3}H-thymidine incorporation, was suppressed upon coculture with CD4⁺CD25⁺CCR4⁺ cells, including Tregs ($n = 3$, $P < 0.01$; Figure 1B). However, after being transduced with lentiviral vector expressing GFP-Tax, the CD4⁺CD25⁺CCR4⁺ cells no longer suppressed cell proliferation; conversely, cells transduced with the control vector expressing only GFP retained full suppressive function ($P < 0.001$; Figure 1B).

The HTLV-1 protein product Tax induces IFN-γ production via T-bet. Experiments were conducted to determine if and how Tax affects IFN-γ production in infected T cells. First, the existence of a functional link between *Tax* and *IFNG* was established by using the

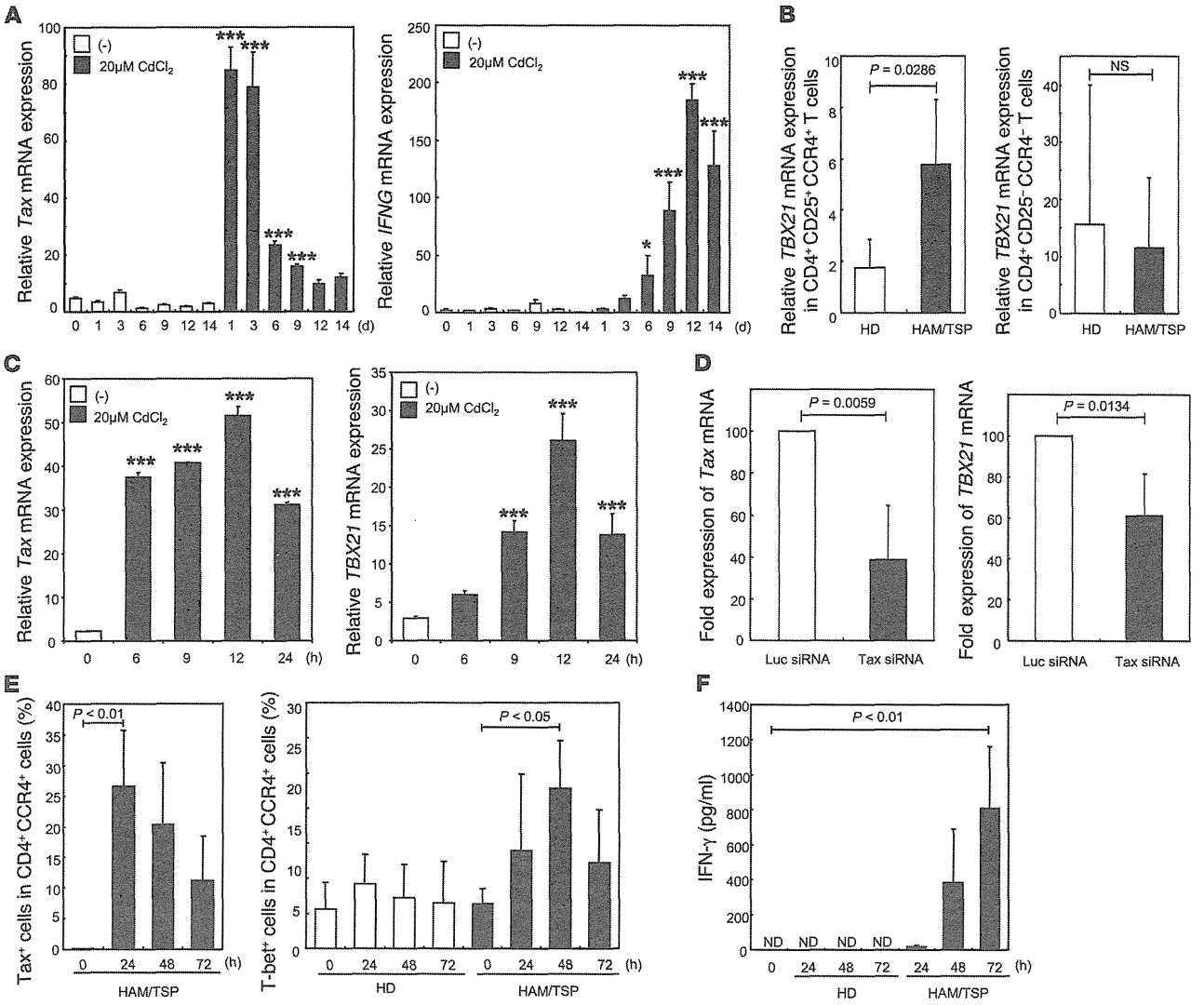

Figure 2. Tax induces IFN-γ production via T-bet. (**A**) Tax-dependent *IFNG* mRNA expression in JPX-9 cells. Experiments were performed in triplicate. (**B**) Elevated *TBX21* mRNA expression in $CD4^+CD25^+CCR4^+$ T cells from HAM/TSP patients relative to HDs ($n = 4$ per group). (**C**) Tax-dependent *TBX21* mRNA expression in JPX-9 cells. Experiments were performed in triplicate. (**D**) Reduced *TBX21* mRNA expression after silencing Tax in $CD4^+CD25^+CCR4^+$ T cells from HAM/TSP patients. PBMCs from HAM/TSP patients ($n = 5$) were FACS sorted, transfected with either Luc or Tax siRNA, and incubated for 24 hours. (**E** and **F**) Tax expression correlated with T-bet expression and IFN-γ production in $CD4^+CCR4^+$ T cells from HAM/TSP patients. $CD4^+CCR4^+$ T cells isolated from HDs and HAM/TSP patients ($n = 4$ per group) were cultured before being stained for Tax and T-bet protein and analyzed using FACS. IFN-γ production in the culture medium was measured using a CBA assay. ND, not detectable. All data are mean ± SD. *P* values were calculated using (**A** and **C**) 1-way ANOVA followed by Dunnett test for multiple comparisons, (**B**) Mann-Whitney *U* test, (**D**) paired *t* test, or (**E** and **F**) Friedman test followed by Dunn test for multiple comparisons. $^*P < 0.05$, $^{***}P < 0.001$ vs. time point 0.

JPX-9 cell line possessing a stably integrated $CdCl_2$-inducible *Tax* construct and measuring *IFNG* mRNA expression. Inducing *Tax* expression with $CdCl_2$ periodically over 2 weeks yielded a steady rise in *IFNG* expression (Figure 2A). Although there was clearly a correlation between Tax and IFN-γ expression, the *IFNG* expression level was not proportional to that of *Tax*, and the steepest rise in the former was delayed several days after the steepest rise in the latter. Thus, we suspected that expression of 1 or more additional genes may represent an important middle step on the pathway linking Tax and IFN-γ production. DNA microarray results revealed that expression of *TBX21*, which is known to be associated with IFN-γ production, was elevated in $CD4^+CD25^+CCR4^+$ cells from the HAM/TSP patient, but not the ATLL patient, compared with the HD (Supplemental Figure 1; supplemental material available online with this article; doi:10.1172/JCI75250DS1). *TBX21* mRNA expression, measured via real-time RT-PCR, was elevated in $CD4^+CD25^+CCR4^+$ cells, but not $CD4^+CD25^-CCR4^-$ cells, from HAM/TSP patients compared with HDs (Figure 2B). A direct correlation between *Tax* and *TBX21* mRNA expression was then established using the JPX-9 cell line, as described above (Figure 2C). Silencing the *Tax* gene with siRNA in $CD4^+CD25^+CCR4^+$ cells from HAM/TSP patients reduced *TBX21* as well as *Tax* expression (Figure 2D). Similarly,

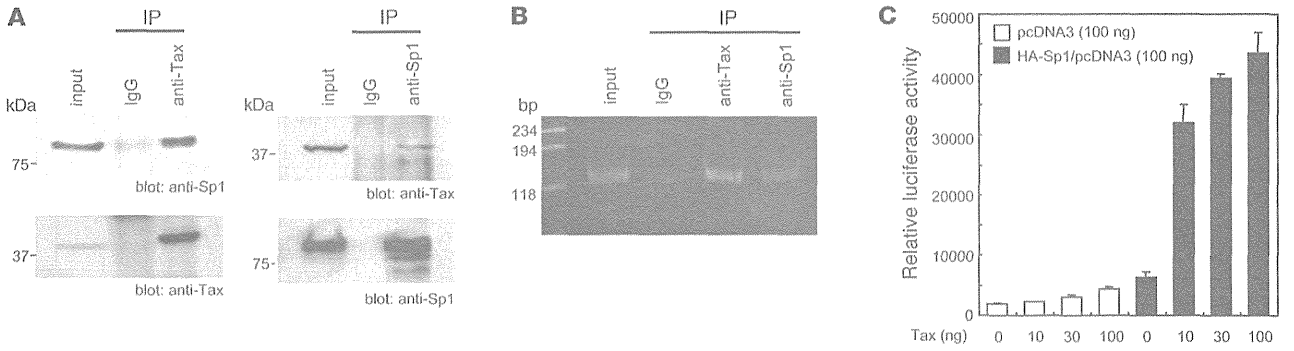

Figure 3. Tax and Sp1 cooperatively enhance *TBX21* promoter activity. (**A**) Co-IP of endogenous Tax and Sp1. Nuclear extracts from MT-2 cells were immunoprecipitated with anti-Tax or anti–Sp1 antibodies or with normal IgG as a control, then immunoblotted with anti-Tax or anti-Sp1 antibodies as indicated. (**B**) Tax bound to the *TBX21* promoter in vivo. ChIP assay using anti-Tax antibody followed by primers encompassing the *TBX21* promoter region (–179 to –59) was performed on genomic DNA isolated from MT-2 cells. DNA (input) and IP with anti-Sp1 served as positive controls, and normal IgG served as a negative control. (**C**) Coactivation of *TBX21* promoter by Sp1 and Tax. HEK293 cells were transfected with 100 ng of *TBX21*-Luc reporter plasmid or Sp1 expression plasmid, as well as 0–100 ng of Tax expression plasmid as indicated. Values were normalized to β-galactosidase activity as an internal control. Data are mean ± SD.

elevation of *Tax* expression via transduction of a GFP-Tax construct into $CD4^+CD25^+CCR4^+$ cells from a HD increased expression of *TBX21* as well as *Tax* (Supplemental Figure 2). Thus, a functional relationship between *Tax* and *TBX21* was confirmed. Finally, among $CD4^+CCR4^+$ cells from HAM/TSP patients, the appearance of Tax^+ cells was associated with a rise in the percentage of $T\text{-}bet^+$ cells, which was associated with a delayed but roughly proportional rise in the amount of IFN-γ protein (Figure 2, E and F). The production of Tax versus T-bet in these $CD4^+CCR4^+$ cells from HAM/TSP patients was compared at 0 versus 48 hours of culturing. At 0 hours, the overwhelming majority of the $CD4^+CCR4^+$ cells were both Tax^- and $T\text{-}bet^-$; by 48 hours, a substantial presence of $Tax^+T\text{-}bet^+$ cells had emerged, and there were very few $T\text{-}bet^+$ cells that were not also Tax^+ (Supplemental Figure 3).

Tax in concert with Sp1 induces TBX21 transcription. Experiments were conducted to investigate the mechanism by which Tax may be involved in *TBX21* transcription in HTLV-1–infected T cells. First, co-IP reactions were performed using nuclear extracts from the HTLV-1–infected MT-2 T cell line to confirm a suspected interaction between endogenous Tax and Sp1, which is known to both form a complex with Tax and to activate *TBX21* transcription (24, 25). Precipitation with anti-Tax or anti-Sp1 antibodies yielded bands corresponding to both Tax and Sp1, whereas precipitation with the nonspecific IgG antibody as the negative control yielded neither band (Figure 3A), thus demonstrating the existence of a Tax-Sp1 complex in HTLV-1–infected T cells. Second, a ChIP assay using primers encompassing the *TBX21* promoter region (–179 to –59) was performed on the MT-2 cells to confirm the suspected interaction between this Tax-Sp1 complex and the *TBX21* promoter. Precipitation with anti-Tax or anti-Sp1, but not IgG, yielded a PCR product corresponding to the *TBX21* promoter (Figure 3B), which suggests that a Tax-Sp1 complex does bind to the *TBX21* promoter site. Finally, a reporter assay was performed using cells transfected with *TBX21*-Luc, a luciferase reporter plasmid containing the *TBX21* promoter region, to confirm a functional relationship among Tax, Sp1, and *TBX21* transcription. Cotransfection with Sp1 resulted in elevated luciferase activity compared with transfection with the reporter alone, and addition of Tax heightened this effect in a concentration-dependent manner (Figure 3C). These findings suggested that Tax, in concert with Sp1, induces *TBX21* transcription.

HTLV-1–infected Th1-like $CCR4^+$ cells are in the CNS of HAM/TSP patients. We next sought to confirm that HTLV-1–infected $CCR4^+$ T cells infiltrate the spinal cords of HAM/TSP patients and exhibit Th1-like traits, such as T-bet and IFN-γ production. Fluorescent immunohistochemical staining of tissue sections from HAM/TSP patient spinal cord lesions revealed the presence of abundant $CCR4^+$ cells infiltrating around the small blood vessels and coexpressing T-bet and IFN-γ (Figure 4A and Supplemental Figure 4). Further investigation revealed that these $CCR4^+$ cells also expressed CXCR3, the marker for Th1 cells (6). It should be noted that both IFN-γ and CXCR3 expression are reported to be induced by T-bet expression (6). Immunofluorescent staining was also used to demonstrate the existence of HTLV-1–infected $CCR4^+$ cells in the CSF of HAM/TSP patients (Figure 4B). $CCR4^+CXCR3^+$ cells were numerous among cells isolated from the CSF of HAM/TSP patients, representing 73.90% of $CD4^+$ cells isolated from a representative patient (Figure 4C) and 63.63% ± 6.73% of $CD4^+$ cells isolated from all patients ($n = 8$; Figure 4D). However, nearly all of these $CD4^+CCR4^+CXCR3^+$ cells were negative for Ki67, a marker of cell proliferation, in the CSF of the HAM/TSP patients (93.94% ± 2.07%, $n = 3$; Figure 4E). The majority of these $CD4^+CCR4^+CXCR3^+$ cells were also $CD25^+$ (70.16% ± 14.08%, $n = 3$, Supplemental Figure 5), confirming the existence of a substantial $CD4^+CD25^+CCR4^+CXCR3^+$ cell population in the CSF of HAM/TSP patients. Importantly, $CD4^+CCR4^+CXCR3^+$ cells did not make up the majority of PBMCs in HAM/TSP patients nor in HDs; in fact, such cells were very few (HAM/TSP, 3.65% ± 1.96%, $n = 8$; HD, 6.88% ± 3.09%, $n = 4$; Figure 4D). PBMCs were also isolated from ATLL patients for comparison, and $CD4^+CCR4^+CXCR3^-$ cells made up the overwhelming majority (83.03% ± 18.61%, $n = 5$; Supplemental Figure 6).

CCR4 shows potential as a molecular target for HAM/TSP immunotherapy. Analysis of HTLV-1 proviral DNA load in subpopulations of $CD4^+$ PBMCs from HAM/TSP patients confirmed that $CCR4^+$ cells were heavily infected, compared with less than

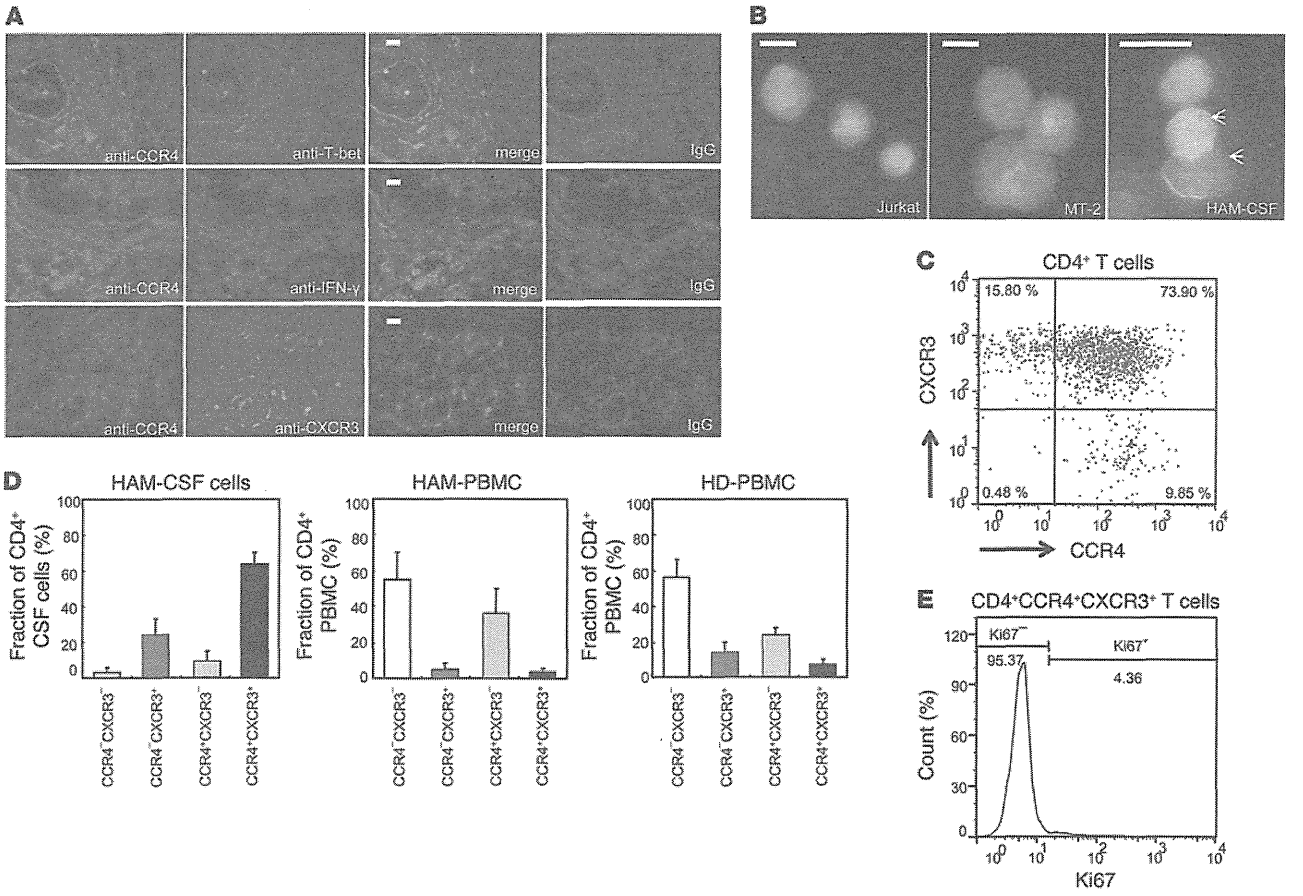

Figure 4. HTLV-1–infected Th1-like CCR4⁺ cells invade the CNS of HAM/TSP patients. (**A**) Detection of CCR4⁺ cells expressing T-bet, IFN-γ, and CXCR3 infiltrating the spinal cord of a HAM/TSP patient. Representative images show immunofluorescent codetection of CCR4 with T-bet, IFN-γ, and CXCR3, as well as the merged images, in thoracic spinal cord sections. Rabbit and goat IgG antibody served as a negative control. Scale bars: 20 μm. (**B**) Presence of HTLV-1–infected CCR4⁺ cells in HAM/TSP patient CSF. Representative images show immunofluorescence-FISH codetection of CCR4 (green) and HTLV-1 provirus (red) in Jurkat cells (uninfected control), MT-2 cells (infected control), and CSF cells from the patients. Arrows denote red provirus signal in the CSF sample. Scale bars: 20 μm. (**C**) CD4⁺ T cells in HAM/TSP patient CSF were mostly CCR4⁺CXCR3⁺. A dot plot of CCR4 and CXCR3 expression in CD4⁺ gated cells isolated from the CSF of a representative HAM/TSP patient is shown. (**D**) CD4⁺CCR4⁺CXCR3⁺ cells were numerous in CSF, but not elevated in peripheral blood, of HAM/TSP patients. Graphs show the percentages of $CCR4^-CXCR3^-$, $CCR4^-CXCR3^+$, $CCR4^+CXCR3^-$ and $CCR4^+CXCR3^+$ T cells among CD4⁺ PBMCs and CSF cells from HAM/TSP patients ($n = 8$) and PBMCs from HDs ($n = 4$). Analysis was performed using FACS. Data are mean ± SD. (**E**) Proliferation was not observed in $CD4^+CCR4^+CXCR3^+$ cells from HAM/TSP patient CSF. The rate of Ki67 expression, a marker for cell proliferation, is shown for $CD4^+CCR4^+CXCR3^+$ gated cells from the CSF of a representative HAM/TSP patient.

1% of $CCR4^-$ cells ($n = 7$; Figure 5A). To predict the efficacy of a CCR4⁺ cell–targeting cytotoxic antibody as a treatment for HAM/TSP, PBMCs were isolated from patients ($n = 9$) and analyzed after being cultured with and without the defucosylated chimeric anti-CCR4 monoclonal antibody KM2760 (21) or, for comparison, the steroid therapy prednisolone (PSL). Addition of 1 μg/ml KM2760 significantly reduced the percentage of CCR4⁺ cells, as measured after 7 days ($P = 0.0039$; Figure 5B). As little as 0.1 μg/ml KM2760 was necessary to reduce the HTLV-1 DNA load ($P < 0.05$), whereas PSL had no significant impact (Figure 5C). Use of 1 μg/ml of either KM2760 or PSL was sufficient to suppress spontaneous proliferation of the PBMCs, as measured by ^{3}H-thymidine incorporation ($P < 0.05$ and $P < 0.01$, respectively; Figure 5D) as well as IFN-γ production ($P < 0.05$ and $P < 0.001$, respectively; Figure 5E). Similar results were observed in experiments using cells isolated from the CSF of HAM/TSP patients ($n = 8$): cultures to which 1 μg/ml of KM2760 had been added exhibited reduced HTLV-1 DNA load ($P = 0.0078$; Figure 5F) and IFN-γ production ($P = 0.0391$; Figure 5G). Certain samples shown in Figure 5G did not exhibit this reduction in IFN-γ production; those samples had particularly low cell counts (0.33–2.00 cells/μl), yielding less reliable data. Despite the presence of those lower-quality samples, statistical significance was still established for the sample group as a whole.

Discussion

Previously, we hypothesized that HTLV-1 gives rise to HAM/TSP by altering the behavior of infected cells via Tax expression to yield a new population of Th1-like proinflammatory cells (26). Evidence indicated that a significant portion of this population might be Tregs, as suggested by the $CD4^+CD25^+CCR4^+$ expres-

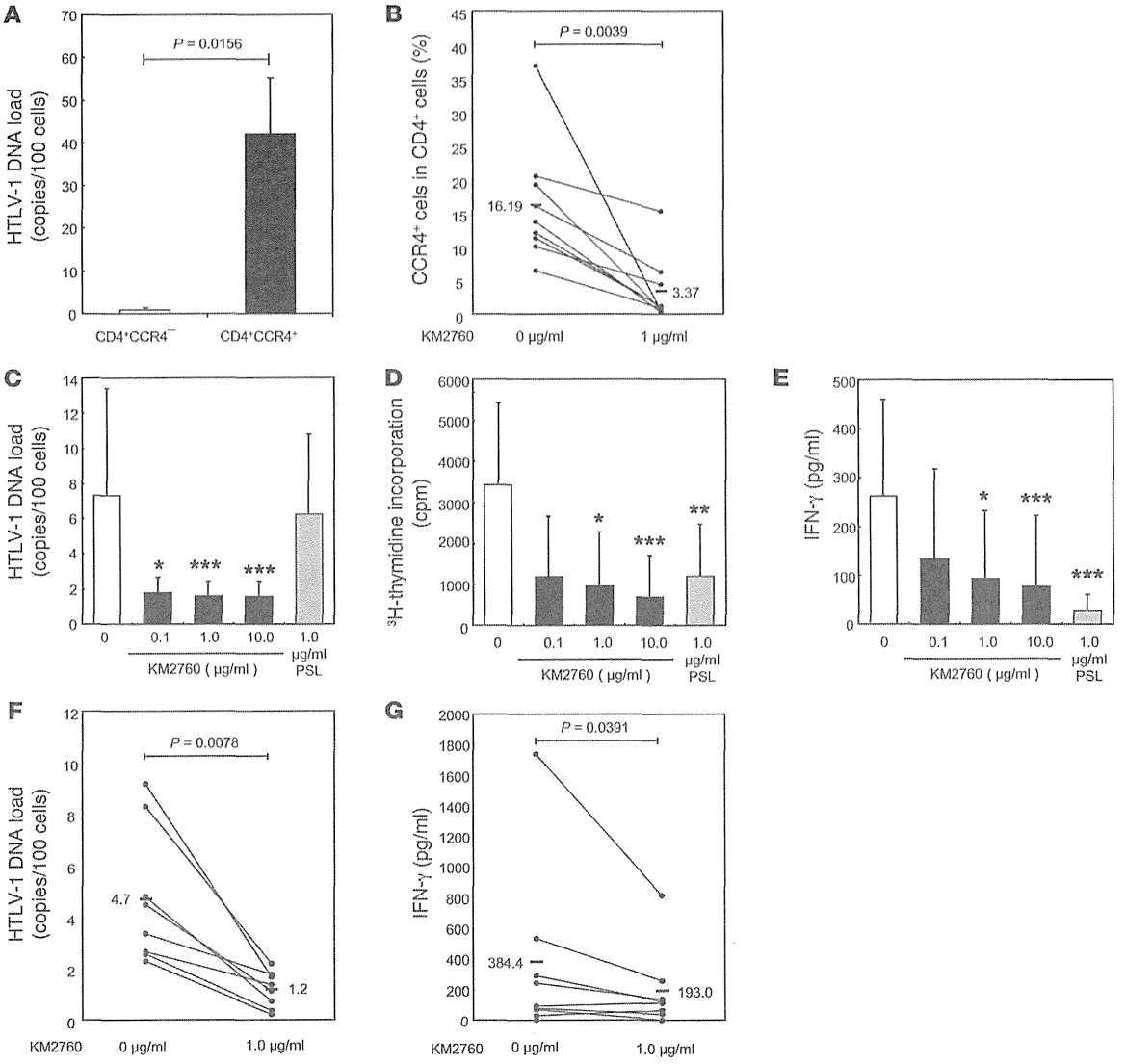

Figure 5. CCR4 shows potential as a molecular target for HAM/TSP immunotherapy. (**A**–**G**) Cells isolated from HAM/TSP patients were sorted via FACS (**A**; $n = 7$) or cultured for 7 days under the following conditions: PBMCs were cultured with various concentrations of KM2760 or 1 μg/ml PSL (**B**–**E**; $n = 9$), and CSF cells were cultured with 1 μg/ml KM2760 (**F** and **G**; $n = 8$). (**A**, **C**, and **F**) HTLV-1 proviral DNA loads were measured using quantitative PCR. (**D**) Degree of spontaneous proliferation was assessed by measuring ^{3}H-thymidine incorporation. (**E** and **G**) IFN-γ production in the culture media was evaluated using CBA assays. HTLV-1 resided in $CD4^+CCR4^+$ rather than $CCR4^-$ cells among PBMCs (**A**), and KM2760 treatment effectively targeted these cells (**B**). Consequently, KM2760 treatment successfully reduced HTLV-1 proviral DNA load (**C**), suppressed spontaneous proliferation (**D**), and decreased IFN-γ production (**E**) in PBMC cultures as well as reducing HTLV-1 DNA load (**F**) and IFN-γ production (**G**) in CSF cell cultures derived from HAM/TSP patients. (**A** and **C**–**E**) Data are mean ± SD. (**B**, **F**, and **G**) Thick horizontal bars represent mean value for all patients; line segments represent individual patients. Statistical analyses were performed using Friedman test followed by Dunn test for multiple comparisons (**C**–**E**) or Wilcoxon test (**A**, **B**, **F**, and **G**). $^*P < 0.05$, $^{**}P < 0.01$, $^{***}P < 0.001$ vs. untreated control.

sion profile (19). We suspected that these infected cells may infiltrate the CNS and trigger an inflammatory positive feedback loop, ultimately leading to chronic spinal cord inflammation (27). In the present study, we provided concrete evidence to support these theories on HAM/TSP pathogenesis, with a particular emphasis on the mechanism by which Tax can induce a proinflammatory phenotype intracellularly via transcriptional regulation.

There is strong evidence to support the conclusion that a substantial portion of the Treg population in HAM/TSP patients is infected with HTLV-1 (28, 29). In a previous study, we demonstrated that $CD4^+CD25^+CCR4^+$ cells were the main reservoir for HTLV-1 in HAM/TSP patients (19), but that expression profile is not exclusive to Tregs. Our present observation that $CD4^+$ T cells positive for FOXP3, a well-established marker for Tregs (10), were more thoroughly infected than the $GATA3^+$ subgroup (Figure 1A) strengthens the argument that Tregs may be the main viral reservoir. It remains debatable whether the virus preferentially infects these cells, promotes their survival (30), or even induces the expression of these

markers. One report postulates that HTLV-1 preferentially infects $CCR4^+$ cells by upregulating CCL22 to encourage cell-to-cell transfer via chemotactic attraction (31). More research is necessary to determine the true mechanism by which infected $CCR4^+$ and $FOXP3^+$ cells become so abundant in HAM/TSP patients.

We demonstrated that the suppressive ability of $CD4^+CD25^+CCR4^+$ cells that characterizes Treg function was impaired by expression of the Tax protein, encoded in the pX region of the HTLV-1 genome (Figure 1B). Prior evidence indicates that Tax may exert these effects via downregulation of FOXP3 expression (20, 32). Transgenic mice expressing Tax exhibit reduced $CD4^+CD25^+FOXP3^+$ Tregs (33) and develop arthritis (34), and transgenic rats expressing HTLV-1 env-pX develop destructive arthropathies, Sjogren syndrome, vasculitis, and polymyositis (35). Collectively, these observations suggest that Tax expression can lead to inflammatory disease by weakening immune tolerance and disrupting homeostasis.

It has long been suspected that in addition to reducing FOXP3 expression, Tax may have the ability to induce IFN-γ production, thereby converting once-suppressive cells into proinflammatory cells. Indeed, intracellular Tax expression has been associated with the rapid upregulation of IFN-γ in infected cells, and researchers have theorized that this upregulation may contribute to the pathogenesis of HTLV-1–associated inflammatory disorders, including HAM/TSP (19, 36, 37). Here we showed at the mRNA level that *Tax* expression stimulated *IFNG* expression; moreover, the effect appeared delayed (Figure 2A), in a manner suggestive of 1 or more intermediate steps in the pathway, rather than direct transcriptional activation. Several candidate pathways have been proposed— such as via NF-κB, STAT1, or STAT5 — but none have been confirmed experimentally (38, 39).

We provided convincing evidence that Tax induces IFN-γ production in infected cells indirectly by amplifying the effects of Sp1 binding to — and increasing the activity of — the *TBX21* promoter: the resulting amplification of T-bet expression was responsible for the rise in IFN-γ production.

T-bet is said to be a Th1-specific T box transcription factor that controls the expression of the hallmark Th1 cytokine, IFN-γ (6). *TBX21*-deficient mice exhibit greater resistance to a variety of inflammatory and autoimmune diseases than their wild-type counterparts (40). Thus, it has been of interest that elevated *TBX21* levels have been found in the PBMCs of HAM/TSP patients (41). We showed that *TBX21* expression was elevated in the $CD4^+CD25^+CCR4^+$ cells of HAM/TSP patients, but not ATLL patients (Figure 2B and Supplemental Figure 1), which suggests that this trait is specific to HAM/TSP pathogenesis. Furthermore, we interpreted the lack of elevation in $CD4^+CD25^-CCR4^-$ cells to indicate that elevated *TBX21* is characteristic of infected cells. Importantly, we clearly demonstrated for the first time that Tax induced T-bet expression (Figure 2, C and E, and Supplemental Figures 2 and 3). Moreover, we showed that this pathway was active in $CD4^+CD25^+CCR4^+$ cells of HAM/TSP patients by silencing Tax expression and observed a corresponding reduction in *TBX21* expression; in the reverse scenario, inducing Tax expression in otherwise-normal $CD4^+CD25^+CCR4^+$ cells from HDs resulted in heightened *TBX21* expression (Figure 2D and Supplemental Figure 2). Finally, we confirmed that this correlation extended to protein production and clearly showed how Tax induces T-bet and subsequently IFN-γ production over time in culture (Figure 2E).

Tax has been reported to stably bind Sp1, a known positive transcriptional regulator of *TBX21* (25, 42). More specifically, interaction with Tax is thought to increase the DNA binding activity of Sp1 (42). Here we used co-IP with samples from the HTLV-1–infected MT-2 cell line to show that endogenous Tax interacted with Sp1 (Figure 3A). Subsequently, ChIP assays revealed that both Sp1 and Tax associated with the *TBX21* promoter region (Figure 3B), a novel finding that supports our theory that Tax and Sp1 together activate *TBX21* transcription. Finally, we showed that in the absence of Sp1, Tax had no significant effect on *TBX21* expression; however, in the presence of Sp1, Tax induced *TBX21* expression in a concentration-dependent manner (Figure 3C). This finding further substantiates our claim that Tax does not directly bind the promoter, but rather acts via Sp1. It should be noted that Tax may induce *TBX21* expression via multiple pathways: it has been reported that Tax enhances STAT1 gene expression in HTLV-1–transformed T cell lines and $CdCl_2$-stimulated JPX-9 cells (38), which suggests that Tax may also induce *TBX21* expression indirectly via STAT1.

The presence of T cell infiltrates in the CNS, indicative of spinal cord inflammation, is a well-known feature of HAM/TSP. Researchers have worked to characterize these cells over the years; together, their findings suggest that the infiltrates are dominated by $CD4^+$ T cells with relatively high proviral loads and elevated Tax and IFN-γ expression (43–45). We hypothesized that a substantial portion of the infiltrate may be made up of infected $CD4^+CCR4^+$ T cells exhibiting Th1-like properties, including IFN-γ production. We used immunohistochemistry to investigate this theory and were able to establish the presence of $CD4^+CCR4^+CXCR3^+$T-$bet^+IFN\text{-}\gamma^+$ cells in spinal cord tissue and HTLV-1–infected $CCR4^+$ cells in the CSF of HAM/TSP patients (Figure 4, A and B). We used FACS analysis to confirm that $CD4^+CCR4^+CXCR3^+$ cells made up the majority of the $CD4^+$ T cells in the HAM/TSP patient CSF (Figure 4C). For the sake of continuity between this and our previous study (19), we also confirmed that the majority of these $CD4^+CCR4^+CXCR3^+$cellswerealso$CD25^+$(SupplementalFigure5), further suggestive of a Treg identity.

We interpret the observation that these $CD4^+CCR4^+CXCR3^+$ cells were virtually nonexistent among PBMCs in HAM/TSP patients (Figure 4D) to mean that the cells had migrated to the CNS, leaving few behind in the periphery. The surprising observation that the Ki67 marker for cell proliferation was negative in the overwhelming majority of $CD4^+CCR4^+CXCR3^+$ cells in the CSF (Figure 4E) signifies that the cells are indeed proliferating elsewhere and subsequently migrating to the CNS. It has in fact been said that HTLV-1–infected cells may be extraordinarily capable of crossing the blood-brain barrier (46). Due to the high proportion of CCR4 positivity among HTLV-1–infected cells (19), the high proviral load in the CSF of HAM/TSP patients (47), and the elevated levels of CCL22 in HAM/TSP patient peripheral blood (30), one might hypothesize that the infected cells migrate across the blood-brain barrier in response to chemokine ligands of CCR4, namely CCL22. However, we found that the CSF of HAM/TSP patients contained only negligible amounts of CCL22, instead favoring the CXCR3 ligand CXCL10 (48). We now postulate that

$CD4^+CCR4^+CXCR3^+$ T cells and other $CXCR3^+$ cells may migrate to the CNS via chemotaxis induced by CXCL10 secreted by astrocytes in the CNS. Previously, we showed that these astrocytes produce CXCL10 in response to IFN-γ, and these levels are further amplified by the invading $CXCR3^+$ cells (27). Together, these findings indicate that a positive feedback loop involving the recruitment of proinflammatory cells to the CNS is the source of chronic inflammation in HAM/TSP, and that the original trigger is the migration of IFN-γ–producing HTLV-1–infected cells to the CNS. Where these proinflammatory cells are primarily proliferating, and why they proliferate at different rates in different settings, are questions to be addressed in future studies.

Our findings in this and previous studies imply that targeting $CCR4^+$ cells could constitute an effective treatment for HAM/TSP. Indeed, this strategy is already in play for ATLL patients, the majority of whom suffer from $CCR4^+$ T cell–derived cancers (7). The humanized defucosylated anti-CCR4 monoclonal antibody KW-0761, which has been shown to induce CCR4-specific ADCC, has been approved as a treatment for ATLL (49, 50). The observation that the majority of infected $CD4^+$ PBMCs in HAM/TSP patients were $CCR4^+$ (Figure 5A) suggests that an anti-CCR4 antibody with ADCC properties might be used to effectively treat HAM/TSP patients as well. Steroids are currently the standard of care for HAM/TSP patients, but this approach is not considered optimal: as with many nonspecific treatments, the effectiveness is limited, and the side effects are numerous (51). Here we compared the effects of the defucosylated chimeric anti-CCR4 monoclonal antibody KM2760 (21) with those of the steroid PSL on ex vivo cultures of cells from HAM/TSP patients. Although PSL had more potent effects per microgram, both treatments successfully reduced cell proliferation and IFN-γ production (Figure 5, D, E, and G). In addition, even a small dose of the antibody effectively reduced proviral load, whereas PSL treatment had no significant effect (Figure 5, C and F). These findings support the main premise of this paper, namely, that $CCR4^+$ cells are major viral reservoirs and producers of IFN-γ. Our study is the first to test the effects of such an antibody-based treatment on cells from HAM/TSP patients; the results were promising, and a clinical trial investigating the in vivo effectiveness in HAM/TSP patients is now underway. Importantly, our research indicates that even if the antibody does not cross the blood-brain barrier, it could be therapeutically effective against spinal cord inflammation by eliminating the proinflammatory $CCR4^+$ cells in the peripheral blood that would have migrated to the CNS.

Until very recently, there had been no reports of T cell character changing from suppressive to inflammatory in response to internal transcriptional alterations induced intracellularly by viral products. There have been many reports of Tregs transforming in the presence of inflammation due to the influence of cytokines, including instances where FOXP3 expression is lost and even cases where IFN-γ production is gained (12, 13). The only report of a similar phenomenon occurring via an intracellular virus-induced pathway states that the HTLV-1 basic leucine zipper (HBZ) gene product can reduce the expression of FOXP3 in HBZ-transgenic mouse Tregs (52). Here we showed for the first time that the HTLV-1 virus can similarly affect gene expression in human cells, inducing IFN-γ production, as well as reduce suppressive function. Collectively, the research to date suggests that HTLV-1 may preferentially infect $CCR4^+$ cells, including Tregs, and induce transcriptional changes via Tax that not only reduce FOXP3 expression, but also induce T-bet expression and consequently IFN-γ production, yielding a proinflammatory immune imbalance. While there is considerable evidence to support this theory, further experiments are necessary to prove that this pathway is indeed the origin of HAM/TSP chronic inflammation. However, here we have directly shown that the HTLV-1 protein product Tax can induce the expression of the Th1 master transcription factor T-bet, which certainly implies that HTLV-1 is capable of activating inherent plasticity in T cells and shifting their gene expression profiles toward a Th1-like state.

Methods

Patient selection and sample preparation. The study included HTLV-1–noninfected HDs ($n = 8$, 4 male and 4 female; mean age, 36 yr), asymptomatic carriers ($n = 6$, 4 male and 2 female; mean age, 56 yr), ATLL patients ($n = 6$, 2 male and 4 female; mean age, 68 yr), and HAM/TSP patients ($n = 31$, 9 male and 22 female; mean age, 61 yr). Diagnosis of ATLL was based on the criteria established by Shimoyama (53). HTLV-1 seropositivity was determined by a particle agglutination assay (Serodia-HTLV-1) and confirmed by Western blot (SRL Inc.). HAM/TSP was diagnosed according to WHO guidelines (54).

Samples of PBMCs were prepared using density gradient centrifugation (Pancoll; PAN-Biotech) and viably cryopreserved in liquid nitrogen (Cell Banker 1; Mitsubishi Chemical Medience Corp.). CSF samples were taken from 17 HAM/TSP patients. CSF cells were isolated by centrifugation and cryopreserved in the aforementioned freezing medium until use. Thoracic spinal cord tissue samples from 1 HAM/TSP patient were obtained postmortem, fixed in 10% formalin, and embedded in paraffin.

Antibodies. For FACS studies, labeled anti-CD3 (UCHT1), anti-CD4 (OKT4), anti-GATA3 (TWAJ), and anti-FOXP3 (PCH101) were purchased from eBioscience, and labeled anti-CCR4 (1G1), anti-CD25 (BC96), anti-CXCR3 (1C6), anti–T-bet (4B10), and anti-Ki67 (B56) were purchased from BD Biosciences. For IP studies, anti-Sp1 (PEP2) and normal IgG were purchased from Santa Cruz Biotechnology Inc., and anti-Tax (Lt-4) was prepared as described previously (55). For immunofluorescence studies, anti-CCR4, anti-IFN-γ, and anti-CXCR3 were purchased from Abcam; anti–T-bet was purchased from Santa Cruz Biotechnology Inc.; and Alexa Fluor 488– and Alexa Fluor 594–conjugated secondary antibodies were purchased from Invitrogen. Kyowa Hakko Kirin Co. Ltd. provided KM2760, a chimeric anti-CCR4 IgG1 monoclonal antibody (21).

Plasmids. The *TBX21*-Luc reporter gene plasmid was constructed as described previously (25). The 100-bp promoter fragment (–101 to –1) in the 5′-flanking region of the human *TBX21* gene was obtained by PCR using human PBMC genomic DNA as the template. Primers used for PCR were 5′-CGCCTCGAGGGCGGGGTGGGGCGAGGCGG-3′ and 5′-CCCAAGCTTCTGTCACTAGAGTCGCAGCGCTTT-3′. The amplified PCR product was digested with XhoI/HindIII and cloned into pPicaGene-Basic vector II (Toyo-ink), which yielded *TBX21*-Luc. Creation of the human Sp1 construct with HA-tag added to the N terminus was accomplished via real-time RT-PCR amplification of human PBMC cDNA with the following primers: Sp1 forward, 5′-CGCGAATTCATGAGCGACCAAGATCACTCCATGGA-3′; Sp1 reverse, 5′-CGCCTCGAGTCAGAAGCCATTGCCACTGATATTAATGGAC-3′. The amplified fragment was digested with EcoRI/XhoI and

subcloned into HA-tagged pcDNA3 (Invitrogen). Tax construct with FLAG-tag added to the N terminus was prepared via PCR amplification of template DNA (56) with the following primers: Tax forward, 5′-CGCGAATTCATGGCCCACTTCCCAGGGTTT-3′; Tax reverse, 5′-CGCCTCGAGTCAGACTTCTGTTTCACGGAAATGTTTTTC-3′. The amplified fragment was digested with EcoRI/XhoI and subcloned into FLAG-tagged pcDNA3. The plasmid HTLV-1 provirus (pUC/HTLV-1) was provided by T. Watanabe (University of Tokyo, Tokyo, Japan) (57). A lentiviral vector, CSIICMV, was used as a null expression vector for lentiviral infection (provided by H. Miyoshi, RIKEN BioResource Center, Tsukuba, Japan) (58). CSIICMV/GFP and CSIICMV/GFP-Tax, which express GFP and GFP fused Tax, were constructed by inserting digested GFP and GFP-Tax from pEGFP (Clontech) and pEGFP-Tax, respectively, into CSIICMV.

Flow cytometric analysis. PBMCs and CSF cells were immunostained with various combinations of the following fluorescence-conjugated antibodies that tag cell surface markers: CD3 (UCHT1), CD4 (OKT4), CD25 (BC96), CCR4 (1G1), CXCR3 (1C6). In some experiments, cells were fixed with a staining buffer set (eBioscience), then intracellularly stained with antibodies against T-bet (4B10), FOXP3 (PCH101), and GATA3 (TWAJ). Cells were stained with a saturating concentration of antibody in the dark (4°C, 30 minutes) and washed twice before analysis using FACSCalibur or LSR II (BD Biosciences). Data were processed using FlowJo software (TreeStar). For cell sorting, JSAN (Bay Bioscience) was used, and the purity exceeded 95%.

Cell isolation. $CD4^+CD25^+CCR4^+$ cells, $CD4^+CD25^-CCR4^-$ cells, $CD4^+GATA3^+$ cells, and $CD4^+FOXP3^+$ cells were separated by FACS sorting. $CD4^+$ T cells were isolated from PBMCs using negative selection with magnetic beads (MACS $CD4^+$ T cell isolation kit; Miltenyi Biotec). $CD4^+CCR4^-$ or $CD4^+CCR4^+$ cells were then isolated from these $CD4^+$ T cells using positive selection with anti-CCR4 Ab (1G1) and rat anti-mouse IgG1 microbeads (Miltenyi Biotec).

Cell culture conditions. HEK293 cells were cultured in MEM (Wako Pure Chemical Industries) supplemented with 10% heat-inactivated FBS (Gibco, Invitrogen) and 1% penicillin/streptomycin (P/S) (Wako Pure Chemical Industries). HEK293T cells were cultured in DMEM–high glucose (Sigma-Aldrich) supplemented with 10% FBS and 1% P/S. Jurkat, MT-2, and JPX-9 cells were cultured in RPMI 1640 medium (Wako Pure Chemical Industries) supplemented with 10% FBS and 1% P/S. JPX-9 is a subline of Jurkat carrying Tax under the control of the metallothionein promoter (provided by M. Nakamura, Tokyo Medical and Dental University, Tokyo, Japan) (59), by which Tax expression is inducible by the addition of 20 μM $CdCl_2$ (Nacalai Tesque Inc.). PBMCs, $CD4^+CCR4^+$ cells, $CD4^+CD25^+CCR4^+$ cells, and $CD4^+CD25^-CCR4^-$ cells isolated from HDs or HAM/TSP patients were cultured in RPMI 1640 medium supplemented with 5% human AB serum (Gibco, Invitrogen) and 1% P/S.

Gene expression profiling and analyses. For transcriptional profiling, $CD4^+CD25^+CCR4^+$ T cells from a HAM/TSP patient, an ATLL patient, and an HD were separated using FACS sorting. Total RNA was prepared using ISOGEN (Nippon gene) following the manufacturer's recommendations. RNA was amplified and labeled with cyanine 3 (Cy3) using an Agilent Quick Amp Labeling Kit, 1-color (Agilent Technologies), following the manufacturer's instructions. For each hybridization, Cy3-labeled cRNA were fragmented and hybridized to an Agilent Human GE 4x44K Microarray (design ID 014850). After washing, microarrays were scanned using an Agilent DNA microarray scanner. Intensity values of each scanned feature were quantified using Agilent feature extraction software (version 9.5.3.1), which performs background subtractions. All data were analyzed using GeneSpring GX software (Agilent Technologies). There were a total of 41,000 probes on Agilent Human GE 4x44K Microarray (design ID 014850), not including control probes. Microarray data were deposited in GEO (accession no. GSE57259).

Real-time PCR and real-time RT-PCR. The HTLV-1 proviral DNA load was measured using ABI Prism 7500 SDS (Applied Biosystems) as described previously (19). For real-time RT-PCR analysis, total RNA isolation and cDNA synthesis were performed as described previously (19). Real-time PCR reactions were carried out using TaqMan Universal Master Mix (Applied Biosystems) and Universal Probe Library assays designed using ProbeFinder software (Roche Applied Science). ABI Prism 7500 SDS was programmed to have an initial step of 2 minutes at 50°C and 10 minutes at 95°C, followed by 45 cycles of 15 seconds at 95°C and 1 minute at 60°C. The primers used were as follows: *TBX21*, 5′-TGTGGTCCAAGTTTAATCAGCA-3′ (forward) and 5′-TGACAGGAATGGGAACATCC-3′ (reverse) (probe no. 9; Roche Applied Science); *Tax*, 5′-ATACAACCCCCAACATTCCA-3′ (forward) and 5′-TTTCGGAAGGGGGAGTATTT-3′ (reverse) (probe no. 69; Roche Applied Science). The primers and probes for detecting *Tax*, *IFNG*, and *GAPDH* mRNA were described previously (19). Relative quantification of mRNA was performed using the comparative Ct method using GAPDH as an endogenous control. For each sample, target gene expression was normalized to the expression of GAPDH, calculated as $2^{-(Ct[target]-Ct[GAPDH])}$.

Virus preparation and cell infection. 293T cells (1×10^6) plated in 100-mm dishes were cotransfected with the appropriate lentiviral-GFP or lentiviral–GFP-Tax expression vector (17 μg), vesicular stomatitis virus G expression vector VSV-G (pMD.G) (5 μg), rev expression vector pRSVRev (5 μg), and gag-pol expression vector pMDLg/pRRE (12 μg) (60) using Lipofectamine 2000 (Invitrogen) according to the manufacturer's protocol. After 4 hours, cells were washed 3 times with PBS, 5 ml of new medium was added, and cells were incubated for 48 hours. Culture supernatants were harvested and filtered through 0.45-μm pore size filters. Lentivirus was concentrated approximately 40-fold by low centrifugation at 6,000 *g* for 16 hours and resuspended in 2 ml RPMI 1640 medium. Freshly isolated $CD4^+CD25^+CCR4^+$ T cells were activated using Treg Suppression Inspector (Anti-Biotin MACSiBead Particles preloaded with biotinylated CD2, CD3, and CD28 antibodies) according to the manufacturer's protocol (Miltenyi Biotec). After being cultured for 36 hours, cells were transduced with equal amounts of the GFP or GFP-Tax lentivirus (MOI 15), followed by centrifugation for 1 hour at 780 *g*, 32°C. After being cultured for 4 hours at 32°C, cells were washed with culture medium and cultured in round-bottomed 96-well plates at 37°C.

Treg suppression assay. A study was conducted to compare the capacities of GFP versus GFP-Tax lentivirus–infected $CD4^+CD25^+CCR4^+$ T cells to suppress cell proliferation. T cell samples were taken from HDs, and 5×10^4 $CD4^+CD25^-$ T cells were stimulated with the Treg Suppression Inspector (see above) according to the manufacturer's instructions. These cells were then cocultured with 5×10^4 GFP lentivirus–infected $CD4^+CD25^+CCR4^+$ T cells or GFP-Tax lentivirus–infected $CD4^+CD25^+CCR4^+$ T cells. After culturing for 4 days, cell proliferation was measured using a ^{3}H-thymidine incorporation assay as described previously (19).

RNA interference assay. siRNA was synthesized chemically at Hokkaido System Science. The sequences of siRNA oligonucleotides were as follows: Tax, 5′-GGCCUUAUUUGGACAUUUATT-3′ and 5′-UAAAUGUCCAAAUAAGGCCTT-3′ (31); Luc, 5′-CGUACGCG-GAAUACUUCGATT-3′ and 5′-UCGAAGUAUUCCGCGUACGTT3′. Next, 100 pmol annealed RNA duplex was transfected using Human T cell Amaxa Nucleofector Kit according to the manufacturer's recommendations (Lonza). 100 pmol Luc siRNA was used as a negative control. Cells were incubated for 48 hours and then harvested and subjected to real-time RT-PCR analysis.

Measurement of IFN-γ. IFN-γ concentration in the culture supernatant was measured with a cytometric bead array kit (BD Biosciences) using a FACSCalibur flow cytometer (BD Biosciences) according to the manufacturer's instructions.

IP. Approximately 1 mg of MT-2 nuclear extracts were incubated with 5 μg anti-Tax, anti-Sp1, or normal IgG coupled with protein G–agarose (Roche Applied Science) in IP buffer (10 mM HEPES [pH 7.9], 100 mM KCl, 1 mM EDTA, 1 mM dithiothreitol, 0.1% NP-40, 1 mM Na_3VO_4, 5 mM NaF, 2 μg/ml aprotinin, 2 μg/ml leupeptin, and 2 μg/ml pepstatin) for 2 hours. The precipitated proteins were washed with the IP buffer, separated by 10% SDS-PAGE, and immunoblotted with anti-Tax or anti-Sp1 antibodies.

ChIP assay. ChIP assay was performed using a ChIP assay kit (Upstate Biotechnology) with some modifications. Briefly, 5×10^6 MT-2 cells were fixed with 1% formaldehyde at 37°C for 25 minutes and washed twice with PBS. Cells were subsequently harvested and sonicated in lysis buffer. Precleared chromatin samples were immunoprecipitated with 5 μg anti-Tax antibody, anti-Sp1 antibody, or normal IgG for 16 hours at 4°C. Immune complexes were collected with salmon sperm DNA/protein G–sepharose for 90 minutes with rotation, washed, and then incubated at 65°C for 6 hours for reverse cross-linking. Chromatin DNA was extracted and analyzed using PCR with primers for the *TBX21* promoter region (–179 to –59; forward, 5′-GCCAAGAGCGTAGAATTTGC-3′; reverse, 5′-CGCTTT-GCTGTGGCTTTATG-3′) (25, 61). Amplification was performed using ExTaq (Takara Bio) with 1 cycle at 95°C for 5 minutes followed by 30 cycles of 95°C for 30 seconds, 54°C for 30 seconds, and 72°C for 30 seconds. Amplified products were analyzed using 8% polyacrylamide gel electrophoresis.

Luciferase assay. For transient transfection, HEK293 cells were seeded at 5×10^4 cells/well into 24-well plates. After 12 hours, medium was changed to MEM supplemented with 10% FBS and 1% P/S, and each plasmid was transfected with CellPhect Transfection Kit according to the manufacturer's recommendations (GE Healthcare). 50 ng pRSV-βgal plasmid was included in each transfection experiment to control for the efficiency of transfection. The total amount of transfected DNA was kept constant with pcDNA3 in all samples. After 48 hours, cells were lysed with Passive Lysis Buffer (Promega), and luciferase activity was measured using the Promega luciferase assay system and MicroLumat Plus LB96V (Berthold Technologies). Values were normalized to β-galactosidase activity as an internal control.

Tissue staining. Formalin-fixed thoracic spinal cord tissue sections were deparaffinized in xylene and rehydrated in a series of graded alcohols and distilled water. The antigenicity of the tissue sections was recovered using a standard microwave heating technique. For immunofluorescence, the slides were incubated in PBS with 10% goat serum for 1 hour at room temperature, then in anti-CCR4 antibody, anti–T-bet antibody, anti–IFN-γ antibody, and anti-CXCR3 antibody overnight at 4°C, labeled with Alexa Fluor 488– or Alexa Fluor 594–conjugated secondary antibody, and examined under a fluorescence microscope (Nikon eclipse E600 with fluorescence filter Nikon F-FL; Nikon Instech) with rabbit or goat IgG as the negative control. Tissue sections were also stained with H&E.

Immunofluorescence staining and immunofluorescence-FISH. Jurkat cells, MT-2 cells, and cells from the CSF of 3 HAM/TSP patients were attached to slides using a cytospin centrifuge (Thermo Fisher Scientific) and fixed in 4% paraformaldehyde (Wako Pure Chemical Industries) for 30 minutes. The slides were washed with PBS and then pretreated as follows: slides were immersed in room temperature 0.2M HCl for 20 minutes, followed by 0.2% Triton-X/PBS for 10 minutes, and finally 0.005% pepsin/0.1M HCl heated to 37°C for 5 minutes. After pretreatment, the slides were stained using the immunofluorescence Can Get Signal kit (TOYOBO) according the manufacturer's instructions with anti-CCR4 as the primary antibody and Alexa Fluor 488–conjugated anti-goat IgG as the secondary antibody. After again being fixed with 4% paraformaldehyde, cells were incubated with a nick-translated (Spectrum Red) pUC/HTLV-1 DNA probe, first for 5 minutes at 70°C and then overnight at 37°C. Images were obtained under an automated research microscope (Leica DMRA2) and analyzed with CW4000 FISH software (Leica Microsystems).

Proliferation assay. PBMCs from HAM/TSP patients were plated into 96-well round-bottomed plates (1×10^5 cells/well) and cultured without any mitogenic stimuli. Cell proliferation was measured using a ^{3}H-thymidine incorporation assay as described previously (19).

Statistics. Paired 2-tailed Student's *t* test and Wilcoxon test were used for within-group comparisons. Unpaired 2-tailed Student's *t* test or Mann-Whitney *U* test was used for between-group comparisons. 1-way ANOVA was used for multiple comparisons, followed by Dunnett or Tukey test. Friedman test was used for paired multiple comparisons, followed by Dunn test. Statistical analyses were performed using Graphpad Prism 5 (GraphPad Software Inc.). A *P* value less than 0.05 was considered significant.

Study approval. Written informed consent was obtained from all patients before the study, which was reviewed and approved by the Institutional Ethics Committee at St. Marianna University and conducted in compliance with the tenets of the Declaration of Helsinki.

Acknowledgments

The authors acknowledge the excellent technical assistance provided by Yumiko Hasegawa, M. Koike, Y. Suzuki-Ishikura, and Y. Saito. This work was partly supported by project "Research on Measures for Intractable Disease"; by a matching fund subsidy from the Ministry of Health Labour and Welfare; by JSPS KAKENHI grant nos. 24790898, 25461294, and 25461293; by the Takeda Science Foundation; and by the Daiichi Sankyo Foundation of Life Science.

Address correspondence to: Yoshihisa Yamano, Department of Rare Diseases Research, Institute of Medical Science, St. Marianna University School of Medicine, 2-16-1 Sugao, Miyamae-ku, Kanagawa 216-8512, Japan. Phone: 81.44.977.8111; E-mail: yyamano@marianna-u.ac.jp.

1. Murphy KM, Stockinger B. Effector T cell plasticity: flexibility in the face of changing circumstances. *Nat Immunol*. 2010;11(8):674–680.
2. Cosmi L, Maggi L, Santarlasci V, Liotta F, Annunziato F. T helper cells plasticity in inflammation. *Cytometry A*. 2014;85(1):36–42.
3. Long SA, Buckner JH. CD4+FOXP3+ T regulatory cells in human autoimmunity: more than a numbers game. *J Immunol*. 2011;187(5):2061–2066.
4. Zhou X, Bailey-Bucktrout S, Jeker LT, Bluestone JA. Plasticity of CD4(+) FoxP3(+) T cells. *Curr Opin Immunol*. 2009;21(3):281–285.
5. Hori S, Nomura T, Sakaguchi S. Control of regulatory T cell development by the transcription factor Foxp3. *Science*. 2003;299(5609):1057–1061.
6. Zhu J, Paul WE. CD4 T cells: fates, functions, and faults. *Blood*. 2008;112(5):1557–1569.
7. Ishida T, Ueda R. Immunopathogenesis of lymphoma: focus on CCR4. *Cancer Sci*. 2011;102(1):44–50.
8. Finney OC, Riley EM, Walther M. Phenotypic analysis of human peripheral blood regulatory T cells (CD4+FOXP3+CD127lo/–) ex vivo and after in vitro restimulation with malaria antigens. *Eur J Immunol*. 2010;40(1):47–60.
9. Mjosberg J, Berg G, Jenmalm MC, Ernerudh J. FOXP3+ regulatory T cells and T helper 1, T helper 2, and T helper 17 cells in human early pregnancy decidua. *Biol Reprod*. 2010;82(4):698–705.
10. Williams LM, Rudensky AY. Maintenance of the Foxp3-dependent developmental program in mature regulatory T cells requires continued expression of Foxp3. *Nat Immunol*. 2007;8(3):277–284.
11. Bennett CL, et al. The immune dysregulation, polyendocrinopathy, enteropathy, X-linked syndrome (IPEX) is caused by mutations of FOXP3. *Nat Genet*. 2001;27(1):20–21.
12. Gao Y, et al. Molecular mechanisms underlying the regulation and functional plasticity of FOXP3(+) regulatory T cells. *Genes Immun*. 2012;13(1):1–13.
13. Dominguez-Villar M, Baecher-Allan CM, Hafler DA. Identification of T helper type 1-like, Foxp3+ regulatory T cells in human autoimmune disease. *Nat Med*. 2011;17(6):673–675.
14. Sakaguchi S, et al. Foxp3+ CD25+ CD4+ natural regulatory T cells in dominant self-tolerance and autoimmune disease. *Immunol Rev*. 2006;212:8–27.
15. Viglietta V, Baecher-Allan C, Weiner HL, Hafler DA. Loss of functional suppression by CD4+CD25+ regulatory T cells in patients with multiple sclerosis. *J Exp Med*. 2004;199(7):971–979.
16. Kanangat S, et al. Disease in the scurfy (sf) mouse is associated with overexpression of cytokine genes. *Eur J Immunol*. 1996;26(1):161–165.
17. Lyon MF, Peters J, Glenister PH, Ball S, Wright E. The scurfy mouse mutant has previously unrecognized hematological abnormalities and resembles Wiskott-Aldrich syndrome. *Proc Natl Acad Sci U S A*. 1990;87(7):2433–2437.
18. Clark LB, Appleby MW, Brunkow ME, Wilkinson JE, Ziegler SF, Ramsdell F. Cellular and molecular characterization of the scurfy mouse mutant. *J Immunol*. 1999;162(5):2546–2554.
19. Yamano Y, et al. Abnormally high levels of virus-infected IFN-γ+ CCR4+ CD4+ CD25+ T cells in a retrovirus-associated neuroinflammatory disorder. *PLoS One*. 2009;4(8):e6517.
20. Yamano Y, et al. Virus-induced dysfunction of CD4+CD25+ T cells in patients with HTLV-I-associated neuroimmunological disease. *J Clin Invest*. 2005;115(5):1361–1368.
21. Niwa R, et al. Defucosylated chimeric anti-CC chemokine receptor 4 IgG1 with enhanced antibody-dependent cellular cytotoxicity shows potent therapeutic activity to T-cell leukemia and lymphoma. *Cancer Res*. 2004;64(6):2127–2133.
22. Yoshida M, Seiki M, Yamaguchi K, Takatsuki K. Monoclonal integration of human T-cell leukemia provirus in all primary tumors of adult T-cell leukemia suggests causative role of human T-cell leukemia virus in the disease. *Proc Natl Acad Sci U S A*. 1984;81(8):2534–2537.
23. Cook LB, Rowan AG, Melamed A, Taylor GP, Bangham CR. HTLV-1-infected T cells contain a single integrated provirus in natural infection. *Blood*. 2012;120(17):3488–3490.
24. Zhang L, Zhi H, Liu M, Kuo YL, Giam CZ. Induction of p21(CIP1/WAF1) expression by human T-lymphotropic virus type 1 Tax requires transcriptional activation and mRNA stabilization. *Retrovirology*. 2009;6:35.
25. Yu J, et al. Transcriptional control of human T-BET expression: the role of Sp1. *Eur J Immunol*. 2007;37(9):2549–2561.
26. Araya N, et al. Human T-lymphotropic virus type 1 (HTLV-1) and regulatory T cells in HTLV-1-associated neuroinflammatory disease. *Viruses*. 2011;3(9):1532–1548.
27. Ando H, et al. Positive feedback loop via astrocytes causes chronic inflammation in virus-associated myelopathy. *Brain*. 2013; 136(pt 9):2876–2887.
28. Kohno T, et al. Possible origin of adult T-cell leukemia/lymphoma cells from human T lymphotropic virus type-1-infected regulatory T cells. *Cancer Sci*. 2005;96(8):527–533.
29. Satou Y, Utsunomiya A, Tanabe J, Nakagawa M, Nosaka K, Matsuoka M. HTLV-1 modulates the frequency and phenotype of FoxP3+CD4+ T cells in virus-infected individuals. *Retrovirology*. 2012;9:46.
30. Toulza F, et al. Human T-lymphotropic virus type 1-induced CC chemokine ligand 22 maintains a high frequency of functional FoxP3+ regulatory T cells. *J Immunol*. 2010;185(1):183–189.
31. Hieshima K, Nagakubo D, Nakayama T, Shirakawa AK, Jin Z, Yoshie O. Tax-inducible production of CC chemokine ligand 22 by human T cell leukemia virus type 1 (HTLV-1)-infected T cells promotes preferential transmission of HTLV-1 to CCR4-expressing CD4+ T cells. *J Immunol*. 2008;180(2):931–939.
32. Grant C, Oh U, Yao K, Yamano Y, Jacobson S. Dysregulation of TGF-β signaling and regulatory and effector T-cell function in virus-induced neuroinflammatory disease. *Blood*. 2008;111(12):5601–5609.
33. Ohsugi T, Kumasaka T. Low CD4/CD8 T-cell ratio associated with inflammatory arthropathy in human T-cell leukemia virus type I Tax transgenic mice. *PLoS One*. 2011;6(4):e18518.
34. Iwakura Y, et al. Induction of inflammatory arthropathy resembling rheumatoid arthritis in mice transgenic for HTLV-I. *Science*. 1991;253(5023):1026–1028.
35. Nakamaru Y, et al. Immunological hyperresponsiveness in HTLV-I LTR-env-pX transgenic rats: a prototype animal model for collagen vascular and HTLV-I-related inflammatory diseases. *Pathobiology*. 2001;69(1):11–18.
36. Hanon E, et al. High production of interferon gamma but not interleukin-2 by human T-lymphotropic virus type I-infected peripheral blood mononuclear cells. *Blood*. 2001;98(3):721–726.
37. Yamazato Y, Miyazato A, Kawakami K, Yara S, Kaneshima H, Saito A. High expression of p40(tax) and pro-inflammatory cytokines and chemokines in the lungs of human T-lymphotropic virus type 1-related bronchopulmonary disorders. *Chest*. 2003;124(6):2283–2292.
38. Nakamura N, et al. Human T-cell leukemia virus type 1 Tax protein induces the expression of STAT1 and STAT5 genes in T-cells. *Oncogene*. 1999;18(17):2667–2675.
39. Sun SC, Yamaoka S. Activation of NF-kappaB by HTLV-I and implications for cell transformation. *Oncogene*. 2005;24(39):5952–5964.
40. Lazarevic V, Glimcher LH. T-bet in disease. *Nat Immunol*. 2011;12(7):597–606.
41. Nishiura Y, Nakamura T, Fukushima N, Moriuchi R, Katamine S, Eguchi K. Increased mRNA expression of Th1-cytokine signaling molecules in patients with HTLV-I-associated myelopathy/tropical spastic paraparesis. *Tohoku J Exp Med*. 2004;204(4):289–298.
42. Trejo SR, Fahl WE, Ratner L. The tax protein of human T-cell leukemia virus type 1 mediates the transactivation of the c-sis/platelet-derived growth factor-B promoter through interactions with the zinc finger transcription factors Sp1 and NGFI-A/Egr-1. *J Biol Chem*. 1997;272(43):27411–27421.
43. Furuya T, et al. Heightened transmigrating activity of CD4-positive T cells through reconstituted basement membrane in patients with human T-lymphotropic virus type I-associated myelopathy. *Proc Assoc Am Physicians*. 1997; 109(3):228–236.
44. Moritoyo T, et al. Detection of human T-lymphotropic virus type I p40tax protein in cerebrospinal fluid cells from patients with human T-lymphotropic virus type I-associated myelopathy/tropical spastic paraparesis. *J Neurovirol*. 1999;5(3):241–248.
45. Umehara F, Izumo S, Ronquillo AT, Matsumuro K, Sato E, Osame M. Cytokine expression in the spinal cord lesions in HTLV-I-associated myelopathy. *J Neuropathol Exp Neurol*. 1994;53(1):72–77.
46. Matsuura E, Yamano Y, Jacobson S. Neuroimmunity of HTLV-I Infection. *J Neuroimmune Pharmacol*. 2010;5(3):310–325.
47. Nagai M, Yamano Y, Brennan MB, Mora CA, Jacobson S. Increased HTLV-I proviral load and preferential expansion of HTLV-I Tax-specific CD8+ T cells in cerebrospinal fluid from patients with HAM/TSP. *Ann Neurol*. 2001;50(6):807–812.
48. Sato T, et al. CSF CXCL10, CXCL9, and neopterin as candidate prognostic biomarkers for HTLV-1-associated myelopathy/tropical spastic paraparesis. *PLoS Negl Trop Dis*. 2013;7(10):e2479.
49. Yamamoto K, et al. Phase I study of KW-0761, a defucosylated humanized anti-CCR4 antibody, in relapsed patients with adult T-cell leukemia-lymphoma and peripheral T-cell lymphoma.

J Clin Oncol. 2010;28(9):1591–1598.
50. Ishida T, et al. Defucosylated anti-CCR4 monoclonal antibody (KW-0761) for relapsed adult T-cell leukemia-lymphoma: a multicenter phase II study. *J Clin Oncol.* 2012;30(8):837–842.
51. Yamano Y, Sato T. Clinical pathophysiology of human T-lymphotropic virus-type 1-associated myelopathy/tropical spastic paraparesis. *Front Microbiol.* 2012;3:389.
52. Yamamoto-Taguchi N, et al. HTLV-1 bZIP factor induces inflammation through labile Foxp3 expression. *PLoS Pathog.* 2013;9(9):e1003630.
53. Shimoyama M. Diagnostic criteria and classification of clinical subtypes of adult T-cell leukaemia-lymphoma. A report from the Lymphoma Study Group (1984–1987). *Br J Haematol.* 1991;79(3):428–437.
54. Osame M. Review of WHO Kagoshima meeting and diagnostic guidelines for HAM/TSP. In: Blattner W, ed. *Human Retrovirology: HTLV*. New York, New York, USA: Raven Press; 1990:191–197.
55. Tanaka Y, et al. An antigenic structure of the trans-activator protein encoded by human T-cell leukemia virus type-I (HTLV-I), as defined by a panel of monoclonal antibodies. *AIDS Res Hum Retroviruses.* 1992;8(2):227–235.
56. Yoshiki T, et al. Models of HTLV-I-induced diseases. Infectious transmission of HTLV-I in inbred rats and HTVL-I env-pX transgenic rats. *Leukemia.* 1997;11(suppl 3):245–246.
57. Kamihira S, et al. Intra- and inter-laboratory variability in human T-cell leukemia virus type-1 proviral load quantification using real-time polymerase chain reaction assays: a multi-center study. *Cancer Sci.* 2010;101(11):2361–2367.
58. Bai Y, et al. Effective transduction and stable transgene expression in human blood cells by a third-generation lentiviral vector. *Gene Ther.* 2003;10(17):1446–1457.
59. Nagata K, Ohtani K, Nakamura M, Sugamura K. Activation of endogenous c-fos proto-oncogene expression by human T-cell leukemia virus type I-encoded p40tax protein in the human T-cell line, Jurkat. *J Virol.* 1989;63(8):3220–3226.
60. Dull T, et al. A third-generation lentivirus vector with a conditional packaging system. *J Virol.* 1998;72(11):8463–8471.
61. Shin HJ, Lee JB, Park SH, Chang J, Lee CW. T-bet expression is regulated by EGR1-mediated signaling in activated T cells. *Clin Immunol.* 2009;131(3):385–394.

of Clinical and Translational Neurology
Open Access

RESEARCH ARTICLE

A plasma diagnostic model of human T-cell leukemia virus-1 associated myelopathy

Makoto Ishihara[1], Natsumi Araya[2], Tomoo Sato[2], Naomi Saichi[1], Risa Fujii[1], Yoshihisa Yamano[2] & Koji Ueda[1]

[1]Division of Biosciences, Functional Proteomics Center, Graduate School of Frontier Sciences, The University of Tokyo, Tokyo, Japan
[2]Department of Rare Diseases Research, Institute of Medical Science, St. Marianna University School of Medicine, Kawasaki, Japan

Correspondence
Koji Ueda, Division of Biosciences, Functional Proteomics Center, Graduate School of Frontier Sciences, The University of Tokyo, CREST hall 1F, Institute of Medical Science, 4-6-1 Shirokanedai, Minato-ku, Tokyo, Japan, 108-8639. Tel: +81-3-6409-2062; Fax: +81-3-6409-2063; E-mail: k-ueda@ims.u-tokyo.ac.jp

Funding Information
This work was supported by grant-in-aid for Research Project on Overcoming Intractable Diseases from the Ministry of Health Labour and Welfare Japan and grant-in-aid for Young Scientists (B) (23701090) from the Ministry of Education, Culture, Sports, Science & Technology Japan.

Received: 19 November 2014; Accepted: 9 December 2014

Annals of Clinical and Translational Neurology **2015; 2(3): 231–240**

doi: 10.1002/acn3.169

Abstract

Objective: Human T-cell leukemia virus-1 (HTLV-1) associated myelopathy/tropic spastic paraparesis (HAM/TSP) is induced by chronic inflammation in spinal cord due to HTLV-1 infection. Cerebrospinal fluid (CSF) neopterin or proviral load are clinically measured as disease grading biomarkers, however, they are not exactly specific to HAM/TSP. Therefore, we aimed to identify HAM/TSP-specific biomarker molecules and establish a novel less-invasive plasma diagnostic model for HAM/TSP. **Methods**: Proteome-wide quantitative profiling of CSFs from six asymptomatic HTLV-1 carriers (AC) and 51 HAM/TSP patients was performed. Fourteen severity grade biomarker proteins were further examined plasma enzyme-linked immunosorbent assay (ELISA) assays ($n = 71$). Finally, we constructed three-factor logistic regression model and evaluated the diagnostic power using 105 plasma samples. **Results**: Quantitative analysis for 1871 nonredundant CSF proteins identified from 57 individuals defined 14 CSF proteins showing significant correlation with Osame's motor disability score (OMDS). Subsequent ELISA experiments using 71 plasma specimens confirmed secreted protein acidic and rich in cysteine (SPARC) and vascular cell adhesion molecule-1 (VCAM-1) demonstrated the same correlations in plasma ($R = -0.373$ and $R = 0.431$, respectively). In this training set, we constructed a HAM/TSP diagnostic model using SPARC, VCAM1, and viral load. Sensitivity and specificity to diagnose HAM/TSP patients from AC (AC vs. OMDS 1–11) were 85.3% and 81.1%, respectively. Importantly, this model could be also useful for determination of therapeutic intervention point (OMDS 1–3 + AC vs. OMDS 4–11), exhibiting 80.0% sensitivity and 82.9% specificity. **Interpretation**: We propose a novel less-invasive diagnostic model for early detection and clinical stratification of HAM/TSP.

Introduction

The RNA retrovirus human T-cell leukemia virus-1 (HTLV-1) is endemic in Japan, Caribbean basin, Iran, Africa, South America, and the Melanesian islands.[1] Number of infected individuals is currently estimated at around 30 million worldwide,[2] in which 5% of virus carriers develop HTLV-1 associated myelopathy/tropic spastic paraparesis (HAM/TSP) or adult T-cell leukemia (ATL) after asymptomatic phase of typically over 30 years. Inflammation of spinal cord is a principal symptom of HAM/TSP patients, causing progressive scelotyrbe, gait impairment, or urination disorder.[3] However, no curative therapy for HAM/TSP has been developed except for anti-inflammatory treatments by INF-α or steroids,[4] whereas excessive or long-term use of these drugs can increase the risk of adverse events.[5,6] Hence, the treatment regimens should be carefully managed based on a thorough assessment of disease stage and activity. As for the severity grading of HAM/TSP, Osame's motor disability score (OMDS) is widely used to define disease stages and estimate the rate of disease progression.[7] Although this scale is helpful to evaluate consequential impairment of motor functions, development of molecular-based

diagnostics has been a major challenge for early detection and adequate therapeutic intervention of HAM/TSP.

To identify HAM/TSP-specific biomarkers, a variety of genomic or proteomic analyses were performed for infected T cells and plasma samples,[8-10] however, comprehensive investigation for cerebrospinal fluid (CSF) has not been launched in spite of the most fundamental site of HAM/TSP lesion. Therefore, we intended to acquire the first proteome-wide view of CSFs reflecting HAM/TSP-associated alteration of spinal cord microenvironment. Following the statistical identification of severity grade biomarkers from CSFs, we attempted to construct a HAM/TSP diagnostic model using less-invasive plasma specimens.

Subjects and Methods

Participants

CSF specimens (from 51 HAM/TSP patients and six asymptomatic carriers [ACs]) and plasma specimens (from 50 HAM/TSP patients and 55 ACs) were collected in St. Marianna University School of Medicine and kept frozen at −80°C until just before use. The research procedure was explained and written informed consent was obtained from all the patients. This study was approved by the Ethical Committee of the University of Tokyo (approval code 14-1) and the Ethical Committee of St. Marianna University School of Medicine.

LC/MS/MS analysis

The 20 μL each of CSFs was lyophilized and dissolved in 8 mol/L Urea (GE Healthcare, Buckinghamshire, UK) in 50 mmol/L ammonium bicarbonate (Sigma-Aldrich, St. Louis, MO). After reduction with 5 mmol/L tris(2-carboxyethyl)phosphine (Sigma-Aldrich) at 37°C for 30 min, proteins were alkylated with 25 mmol/L Iodoacetamide (Sigma-Aldrich) at ambient temperature for 45 min. Following fourfold dilution with 50 mmol/L ammonium bicarbonate, proteins were digested with immobilized trypsin (Thermo Scientific, Bremen, Germany) at 37°C for 6 h. Digested samples were then desalted by Oasis HLB μElution plate (Waters, Milford, MA) and analyzed by liquid chromatography - tandem mass spectrometry (LC/MS/MS). The peptides were separated on Ultimate 3000 RSLC nano-HPLC system (Thermo Scientific) equipped with 0.075 × 150 mm C_{18} tip-column (Nikkyo Technos, Tokyo, Japan) using two-step linear gradient comprising 2–35% acetonitrile for 95 min and 35–95% acetonitrile for 15 min in 0.1% formic acid at the flow rate of 250 nL/min. The eluates were analyzed with LTQ Orbitrap Velos mass spectrometer (Thermo Scientific). Spectra were collected using full MS scan mode over the mass-to-charge (m/z) range 400–1600. MS/MS was performed on the top 20 ions in each MS scan using the data-dependent acquisition mode with dynamic exclusion enabled.

2D-LC/MS/MS analysis

CSF tryptic digests were resolved in 10 mmol/L ammonium formate (Sigma-Aldrich) in 25% acetonitrile and fractionated with 0.2 × 250 mm strong cation exchange monolith column (GL Science, Tokyo, Japan). The samples were eluted with the gradient from 10 mmol/L to 1 mol/L of ammonium formate in curve = 3 mode within 70 min using Prominence HPLC system (Shimadzu Corporation, Kyoto, Japan). The eluate was separated into 11 fractions and analyzed by LC/MS/MS.

Protein/peptide identification

MS/MS spectra were searched against SwissProt database version 2012_06 (20,232 human protein sequences) using SEQUEST algorithm on ProteomeDiscoverer 1.3 software (Thermo Scientific). Proteins satisfying the false discovery rate (FDR) <1% by Peptide Validator FDR estimation algorithm on ProteomeDiscoverer was accepted. Gene ontology (GO) term analysis was performed using DAVID Bioinformatics Resources 6.7 (http://david.abcc.ncifcrf.gov/).

Label-free quantification analysis

The LC/MS/MS data from 57 CSF samples were imported on the Expressionist server (Genedata AG, Basel, Swiss) and processed along the workflow shown in Figure S1. The four-step Chromatogram Chemical Noise Subtraction was performed, composed of (1) RT structure removal = true, minimum RT length = 2 scans, (2) m/z structure removal = true, minimum m/z length = 6 scans, (3) RT window = 501 scans, quantile subtraction = 90%, and (4) RT structural removal = true, minimum RT length = 2 scans. Data points with intensity <500 were clipped to zero. Again, Chromatogram Chemical Noise Subtraction was performed using chromatogram smoothing = true, RT windows = 5 scans, and estimator = Moving average. After applying Chromatogram Grid with a distance of scan counts = 10, RT variety among 57 samples was normalized by Chromatogram RT Alignment: m/z windows = 11 points, RT windows = 11 scans, gap penalty = 1, RT search interval = 2 min, alignment scheme = pairwise alignment based tree. Peaks were detected by Chromatogram Summed Peak Detection: summation window = 20 scans, overlap = 10, minimum peak size = 6 scans, maximum merge distance = 1 point,

peak RT splitting = true, intensity profiling = maximum, gap/peak ratio = 5%, refinement threshold = 80, consistency threshold = 1. The detected peaks were grouped in isotopic clusters using Chromatogram Isotopic Peak Clustering: minimum charge = 1, maximum charge = 10, maximum missing peaks = 0, first allowed gap position = 10, RT window = 0.02 min, *m/z* tolerance = 5 ppm, isotope shape tolerance = 10, minimum cluster size ration = 0.5.

Cytometric bead array

Concentration of C-X-C motif chemokine 10 (CXCL10) in CSF was determined by cytometric bead array (CBA) (BD Biosciences, San Jose, CA) according to the manufacturer's instructions.

Enzyme-linked immunosorbent assay

Concentrations of secreted protein acidic and rich in cysteine (SPARC) (R&D Systems, Minneapolis, MN) and vascular cell adhesion molecule-1 (VCAM1) (Abcam, Cambridge, MA) in 105 plasma samples were measured with commercial enzyme-linked immunosorbent assay (ELISA) kit following the manufacturer's instructions. A multivariate logistic regression was applied to construct a new diagnostic model for HAM/TSP utilizing three factors, SPARC, VCAM1, and viral load, as described previously.[11]

Result

Quantitative proteome profiling of CSFs from HAM/TSP patients

CSFs from 6 ACs and 51 HAM/TSP patients (Table 1) were processed according to the schematic workflow of this study (Fig. 1). Nonredundant 68,077 peptides from 57 individuals were detected and quantified on the Expressionist proteome server system, meanwhile 14,451

Table 1. Clinical characteristics of the CSF specimens.

Group	*N*	Age (±SD)	Gender (M/F)
AC	6	55.7 (±15.8)	4/2
HAM1_3	7	57.9 (±14.2)	3/4
HAM4_6	35	59.3 (±11.0)	11/24
HAM7_11	9	61.6 (±8.0)	1/8
Total	57	59.1 (±11.7)	19/38

CSF, cerebrospinal fluid; AC, asymptomatic carriers; HAM1_3, HAM/TSP patients whose Osame's motor disability score from 1 to 3; HAM4_6, HAM/TSP patients whose Osame's motor disability score from 4 to 6; HAM7_11, HAM/TSP patients whose Osame's motor disability score from 7 to 11.

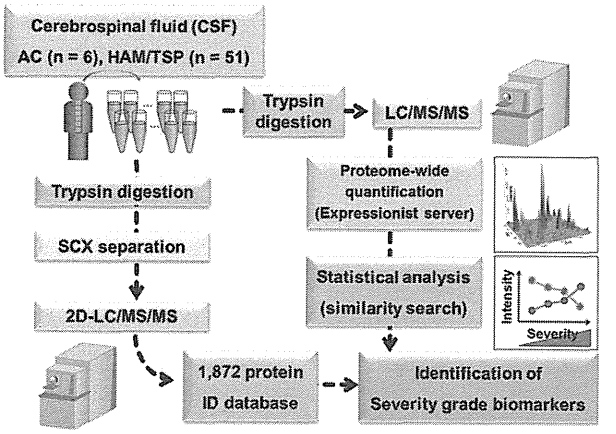

Figure 1. Schematic overview of severity grade marker screening. Cerebrospinal fluids (CSFs) from six asymptomatic carriers (ACs) and 51 HAM/TSP patients were analyzed by LC/MS/MS. Candidate peptides whose intensities had correlation with severity grades were isolated according to Pearson product-moment correlation coefficient. Candidate peptides were identified using Protein/Peptide identification database established by 2D-LC/MS/MS. HAM/TSP, human T-cell leukemia virus-1 associated myelopathy/tropic spastic paraparesis.

CSF peptides (1871 proteins) were identified by parallel 2D-LC/MS/MS analysis. To evaluate quantitative reliability of our LC/MS-based proteome profiling, observed relative concentrations of CXCL10 (Interferon gamma Inducible protein 10, CXCL10) were compared to clinical data which were measured by CBA (Fig. 2A). The result showed strong correlation (R^2 = 0.911) between two measurements, indicating that our LC/MS-based quantification results were highly credible even in the low concentration range (1–20 ng/mL).

Next, to interpret proteome-wide alterations in CSF environment of HAM/TSP patients, 1345 or 1750 proteins identified from AC or HAM/TSP patients group, respectively (Fig. 2B), were classified according to cellular component (CC, Fig. 2C and D) or biological process (BP, Fig. 2E and F) using DAVID Functional Annotation Tool. The CC analysis revealed that proteins expressed in cell projection and plasma membrane were enriched in CSF of HAM/TSP patients, in addition to specific enrichment of viral proteins. This may reflect increased invasive activity of HTLV-1-infected cells into spinal cord, which is often observed in HAM/TSP patients. Further BP analysis indicated that proteins involved in cell adhesion, cell motion, cell migration, cytoskeleton, and cell structure disassembly were highly enriched in CSF of HAM/TSP patients. These features also denoted proteome-wide environmental change in spinal cord, inducing active migration and/or invasion of lymphocytes. Proteins related to cell death and cell growth might associate with spinal inflammation in HAM/TSP patients.

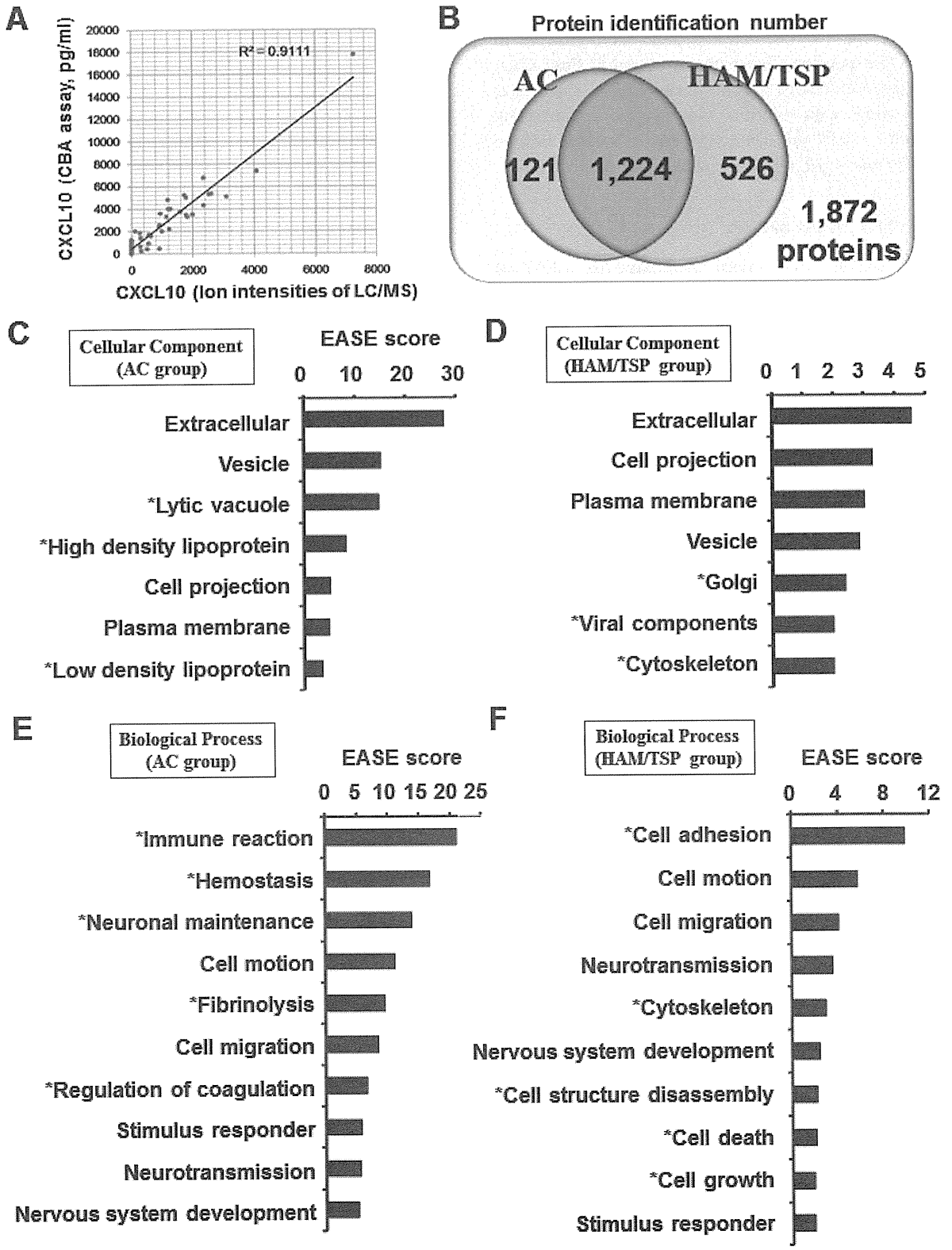

Table 2. List of 16 severity grade markers for HAM/TSP.

UniProt accession	Protein name	Amino acid numbers of identified peptide	Pearson's correlation coefficient (*R*)	*P*-value
Q9NZK5	Adenosine deaminase CECR1	247–258	0.478	5.15E-04
Q12860	Contactin-1	634–647	−0.425	9.94E-04
Q14118	Dystroglycan	222–232	−0.463	2.89E-04
Q8N2S1	Latent-transforming growth factor beta-binding protein 4	310–323	−0.463	2.90E-04
Q9Y5Y7	Lymphatic vessel endothelial hyaluronic acid receptor 1	8–18	−0.499	9.15E-05
Q16653	Myelin-oligodendrocyte glycoprotein	14–25	−0.444	5.40E-04
Q9UJJ9	N-acetylglucosamine-1-phosphotransferase subunit gamma	47–56	−0.442	5.72E-04
P13591	Neural cell adhesion molecule 1	586–597	−0.459	3.31E-04
P36955	Pigment epithelium-derived factor	133–141	−0.454	3.83E-04
Q9UHG2	ProSAAS	14–24	−0.444	5.42E-04
P09486	Secreted protein acidic and rich in cysteine	124–133	−0.523	3.01E-05
P09486	Secreted protein acidic and rich in cysteine	156–164	−0.477	1.75E-04
P09486	Secreted protein acidic and rich in cysteine	252–262	−0.457	3.55E-04
Q92563	Testican-2	139–148	−0.424	1.03E-03
Q06418	Tyrosine-protein kinase receptor TYRO3	279–290	−0.438	1.04E-03
P19320	Vascular cell adhesion protein 1	581–590	0.430	9.35E-04

HAM/TSP, human T-cell leukemia virus-1 associated myelopathy/tropic spastic paraparesis.

Statistical analysis for screening severity grade marker candidates

To extract biomarker proteins showing stoichiometric increase/decrease in accordance with progression of HAM/TSP, numerical classes (0, 1, 2, and 3) were given to four clinically relevant severity groups (AC, HAM/TSP OMDS 1–3, 4–6, and 7–11, respectively) (see Table S1). Then quantitative correlation between severity classes and 68,077 peptide intensities was ranked with Pearson's correlation analysis. Peptides with the lowest 100 *P*-values (Table S2) were next subjected to protein identification analysis by 2D-LC/MS/MS, resulting in successful identification of 14 proteins derived from 16 peptides (Table 2). In addition to Pearson's correlation coefficients and *P*-values in Table 2, LC/MS-based quantitative profiles of 16 peptides were illustrated with box plots (Fig. 3). Compared to a traditional severity grade marker neopterin ($R = 0.4105$, $P = 1.12E\text{-}03$), any of identified proteins showed better potential to be utilized as CSF disease state biomarkers.

SPARC and VCAM-1 as HAM/TSP severity grade markers in plasma

To further narrow down the biomarker candidates and establish plasma-based less-invasive diagnostics, we examined plasma levels of the 14 proteins by ELISA assays measuring 71 training cases (Table 3). The results revealed that a couple of proteins, SPARC and VCAM1, showed the same correlation in plasma with CSF levels ($|R| > 0.4$ and $P < 0.05$) (Fig. 4A and B). Therefore, we attempted construction of the combination biomarker diagnostics using newly identified two proteins and HTLV-1 viral load, all of which are measurable from small volume of blood samples. In order to halt the progression of HAM/TSP and maintain better quality of life for patients, both early diagnosis of HAM/TSP onset and therapeutic intervention at appropriate time point are essential. On the basis of these clinical requirements, we made two logistic regression models which maximized area under the curve (AUC) of ROC curves comparing ACs with HAM/TSP patients (onset predictor; (1)) or

Figure 2. Summary of CSF proteome. (A) Evaluation of LC/MS-based quantification analysis. The relative concentrations of CXCL10 cytokine calculated by mass spectrometric analysis were compared to independent measurements by cytometric bead array (CBA). (B) Venn diagram of identified proteins in 57 CSF analyses. The Gene Ontology (GO) analysis using DAVID Bioinformatics Resources displayed enriched cellular components of CSF proteins in ACs (C) or HAM/TSP patients (D). The enriched biological functions of CSF proteins in ACs (E) or HAM/TSP patients (F) were also shown. Expression Analysis Systematic Explorer (EASE) enrichment scores were shown. CSF, cerebrospinal fluid; CXCL10, C-X-C motif chemokine 10; ACs, asymptomatic carriers; HAM/TSP, human T-cell leukemia virus-1 associated myelopathy/tropic spastic paraparesis.

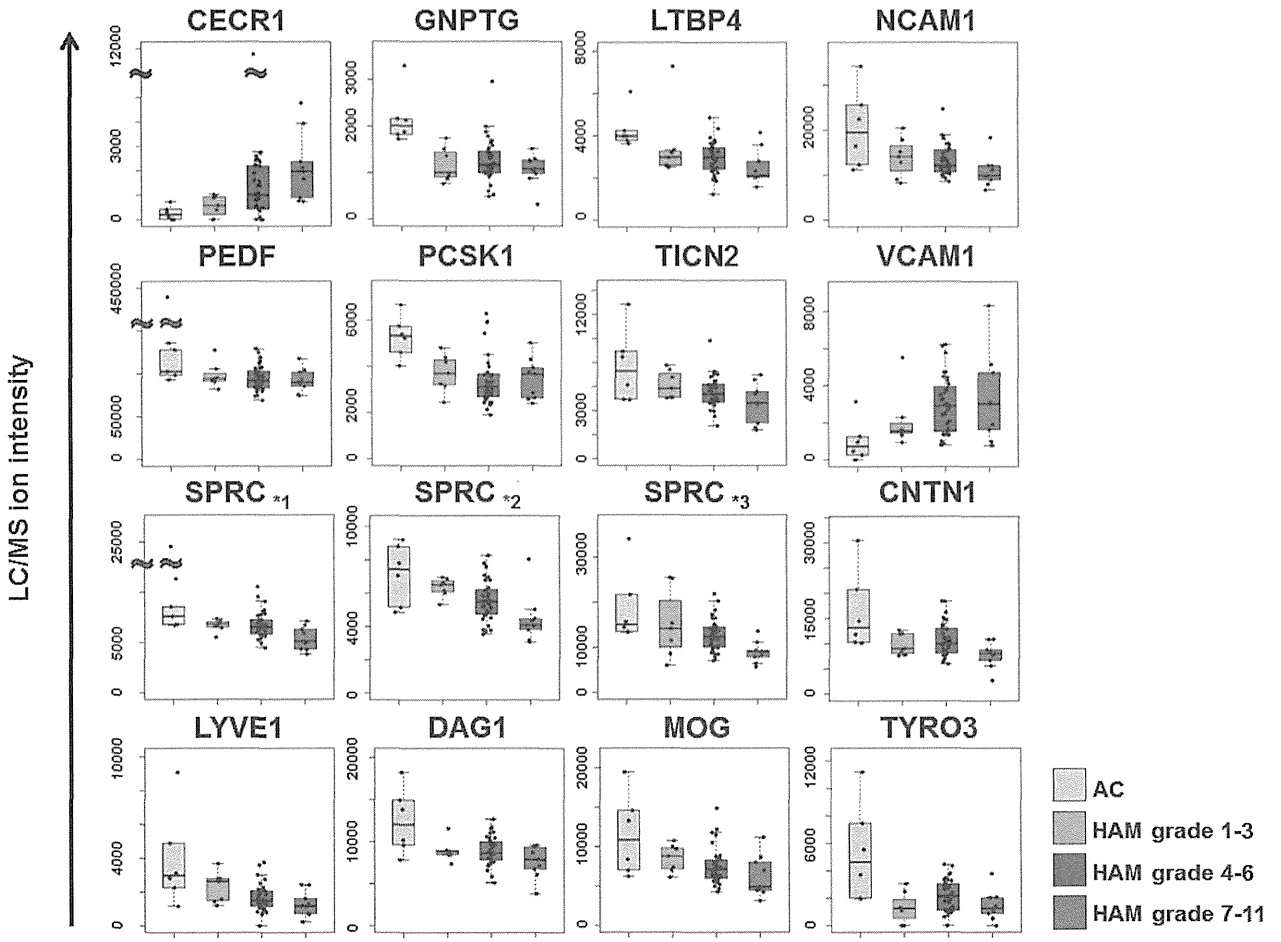

Figure 3. Panels of identified severity grade marker candidates for HAM/TSP. Box plots of 16 peptides derived from 14 candidate proteins are displayed. The Y axis stands for the LC/MS ion intensities. *1, *2, and *3 correspond to distinct SPARC-derived peptides. Amino acid numbers of peptides are as follows: *1; 124–133, *2; 156–164, *3; 252–262. HAM/TSP, human T-cell leukemia virus-1 associated myelopathy/tropic spastic paraparesis; SPARC, secreted protein acidic and rich in cysteine.

Table 3. Clinical characteristics of the plasma specimens.

Group	*N*	Age (±SD)	Gender (M/F)
Training cases			
AC	37	51.5 (±13.2)	13/24
HAM1_3	4	55.0 (±4.7)	3/1
HAM4_6	20	60.5 (±10.8)	4/16
HAM7_11	10	62.0 (±8.2)	2/8
Test cases			
AC	18	54.2 (±12.3)	4/14
HAM1_3	2	59.5 (±12.0)	0/2
HAM4_6	9	56.8 (±14.9)	4/5
HAM7_11	5	71.2 (±2.9)	0/5

AC, asymptomatic carriers; HAM1_3, HAM/TSP patients whose Osame's motor disability score range from 1 to 3; HAM4_6, HAM/TSP patients whose Osame's motor disability score range from 4 to 6; HAM7_11, HAM/TSP patients whose Osame's motor disability score range from 7 to 11.

ACs + HAM/TSP OMDS 1–3 with HAM/TSP OMDS 4–11 (therapeutic intervention predictor; (2)).

$$\log\left(\frac{P(x)}{1-P(x)}\right) = -11.19 - 0.01980\ (\text{SPARC}) + 0.009322\ (\text{VCAM1}) + 0.1142\ (\text{Viral Load}) \quad (1)$$

$$\log\left(\frac{P(x)}{1-P(x)}\right) = -11.73 - 0.01808\ (\text{SPARC}) + 0.009651\ (\text{VCAM1}) + 0.09151\ (\text{Viral Load}) \quad (2)$$

Finally, we assessed our prediction models using 105 plasma samples (71 training samples with 34 independent test samples). The AUC of ROC curves in Figure 4C and D demonstrated significantly higher diagnostic powers of our three-factor models for both onset prediction

